Quantitative Analysis of the Resolved X-ray Emission Line Profiles of O Stars

David Cohen
Department of Physics & Astronomy
Swarthmore College

With Maurice Leutenegger (Columbia), Asif ud-Doula, Rich Townsend, and Stan Owocki (Delaware)

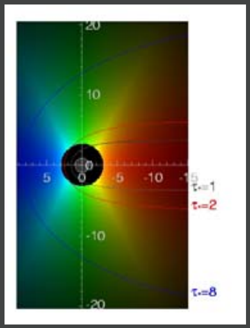

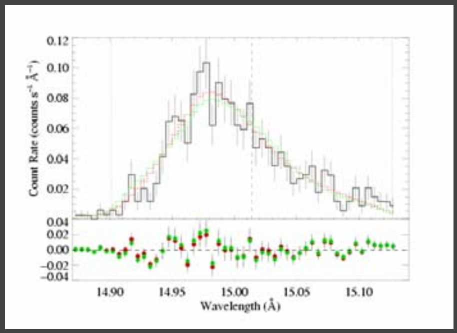

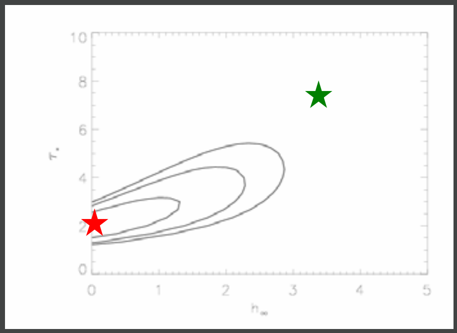

OUTLINE

1. Chandra spectra: emission lines are *broad* and *asymmetric*
2. Hot-star X-rays in context
3. Hot-star winds
4. Emission line shapes: constraints on hot plasma distribution and wind mass-loss rates

Globally, O star X-ray spectra look like coronal spectra

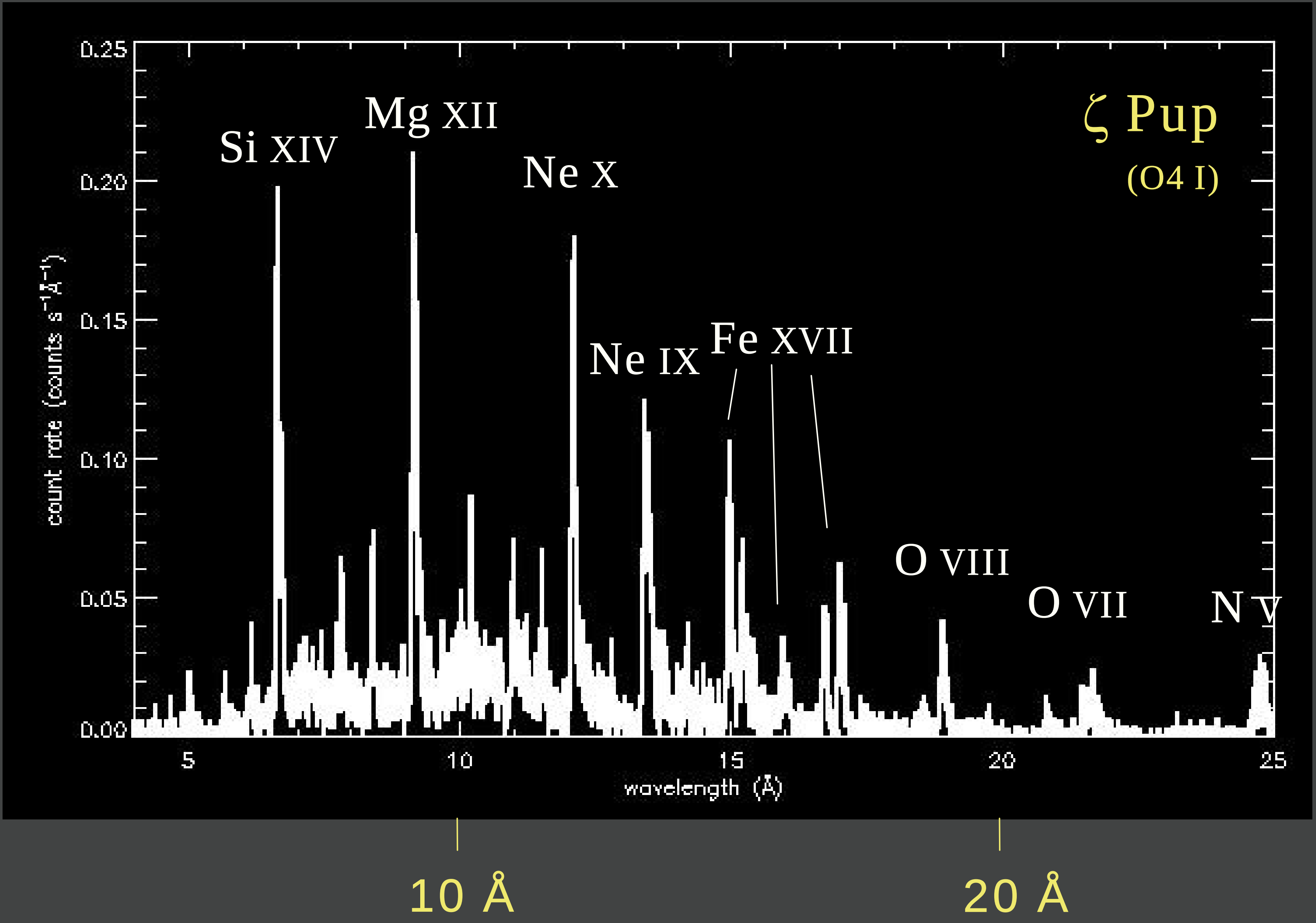

But the emission lines are quite broad

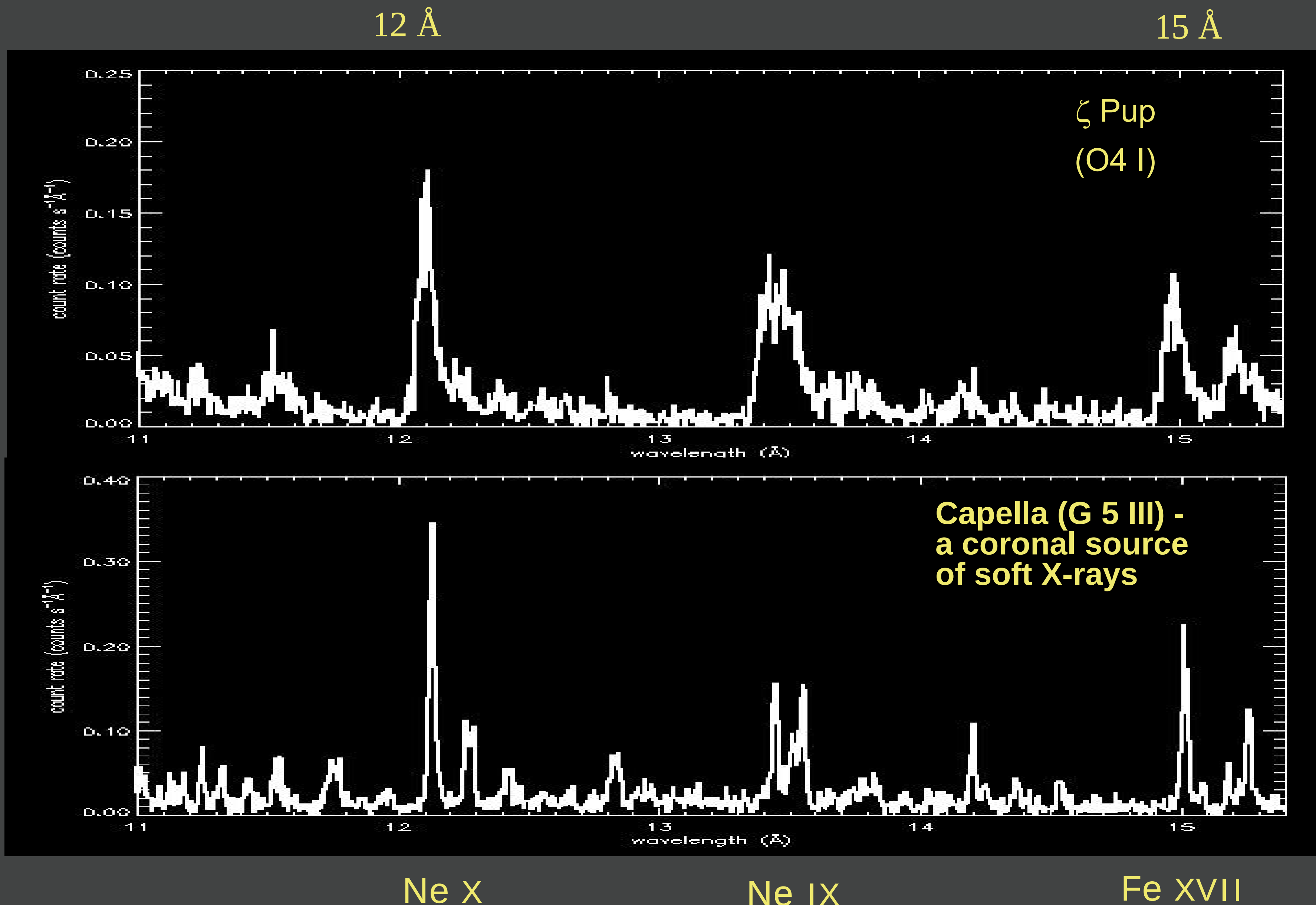

Each individual line (here is Ne X Lyα at 12.13 Å) is significantly Doppler broadened and blue shifted

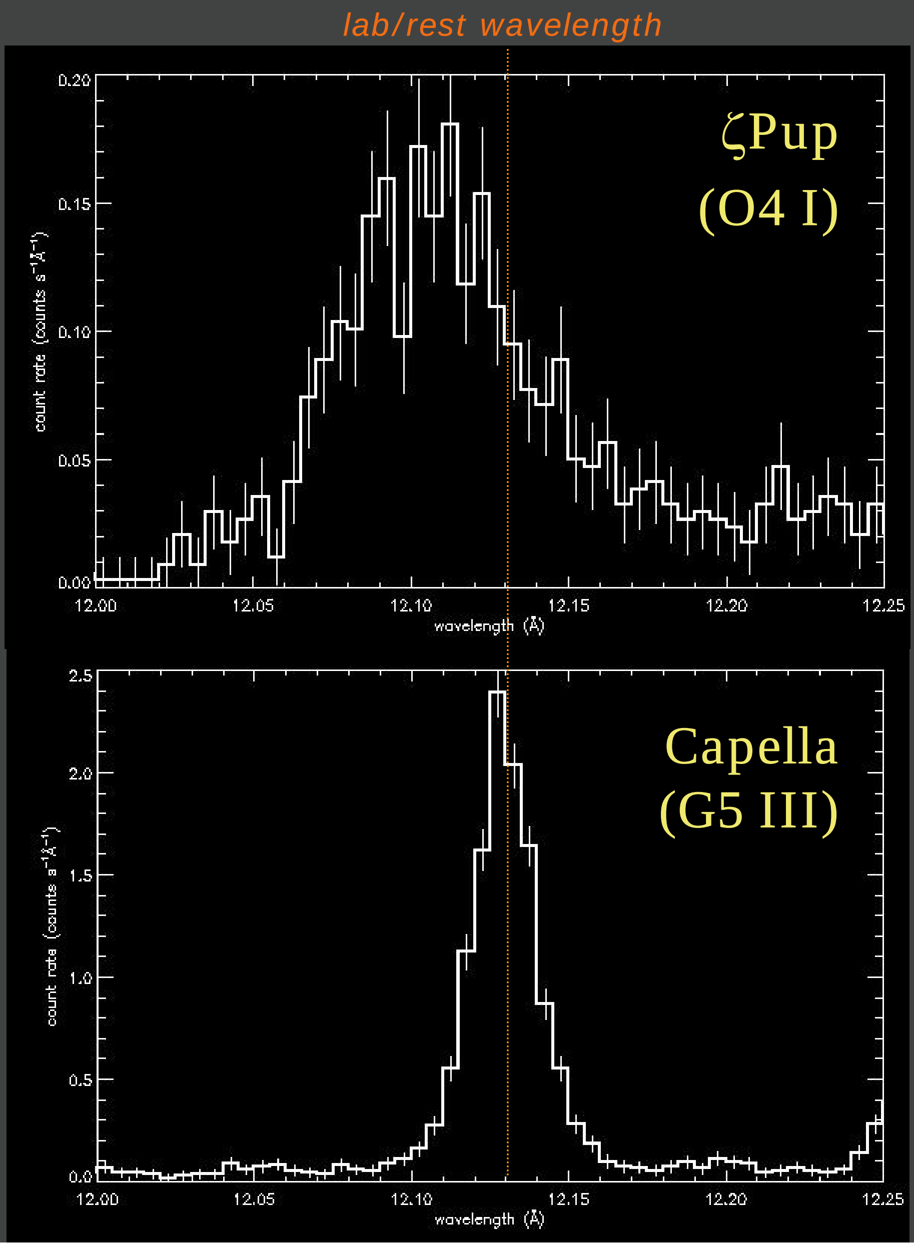

HWHM ~ 1000 km/s

unresolved at MEG resolution

Hot, Massive Stars

Representative properties:

B0 V: T=30,000 K, $M=20M_{sun}$, $L=10^5L_{sun}$

O5 I: T=40,000 K, $M=40M_{sun}$, $L=10^6L_{sun}$

Stars hotter than about 8000 K do ***not*** have convective envelopes: no convection - no dynamo - no hot corona...?

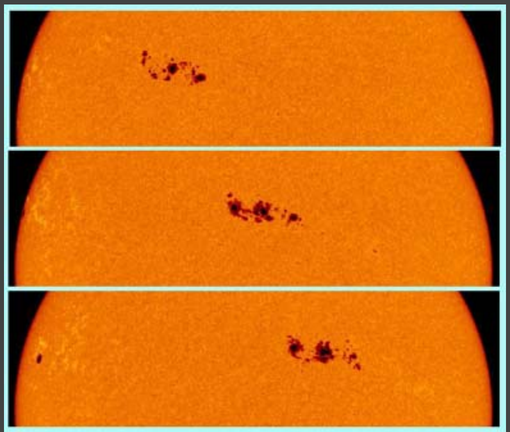

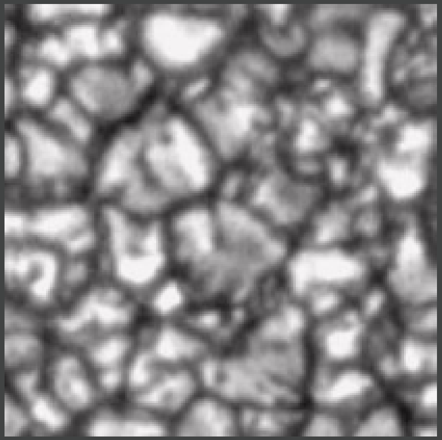

In 1979 the *Einstein Observatory* made the surprising discovery that many O stars are strong X-ray sources

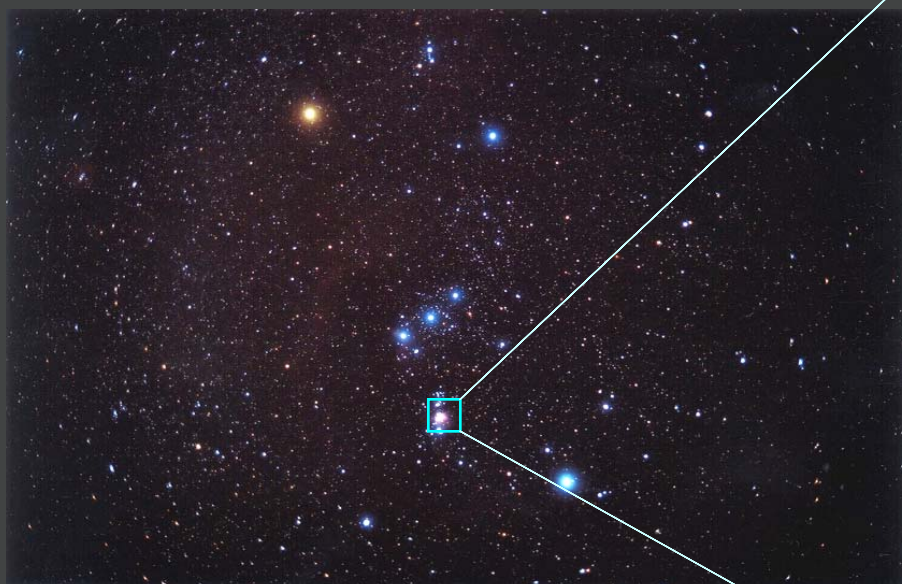

Chandra X-ray image of the Orion star forming region

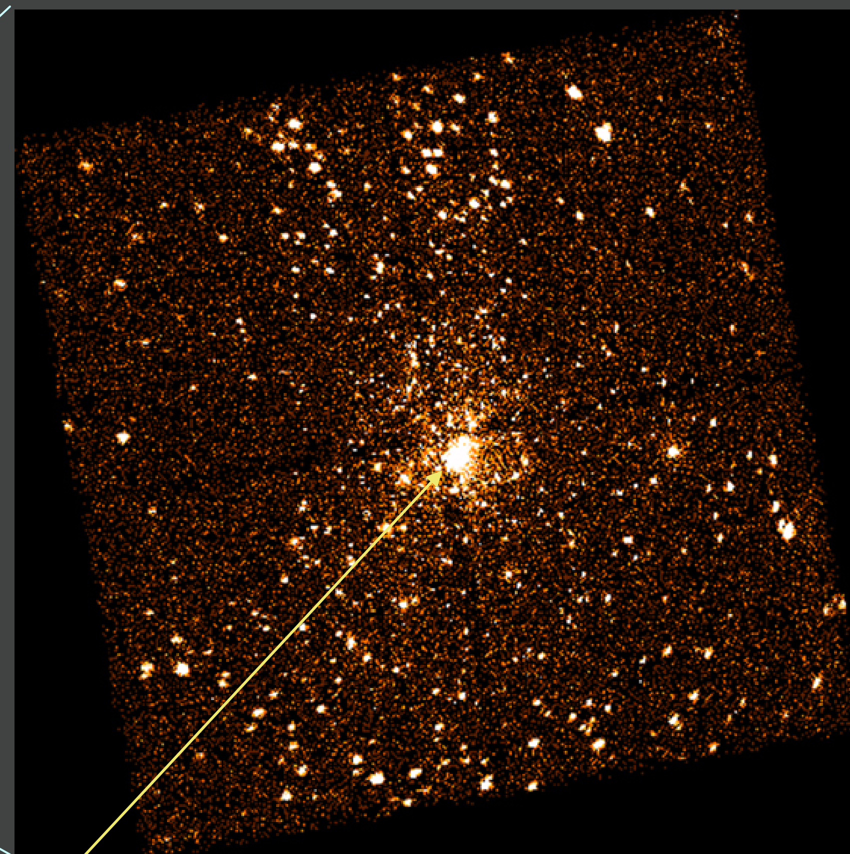

θ^1 Ori C: a T_{eff}=40,000 K
O7 V star (very young, too)

Strong correlation between rotational velocity and x-ray luminosity in solar-type stars

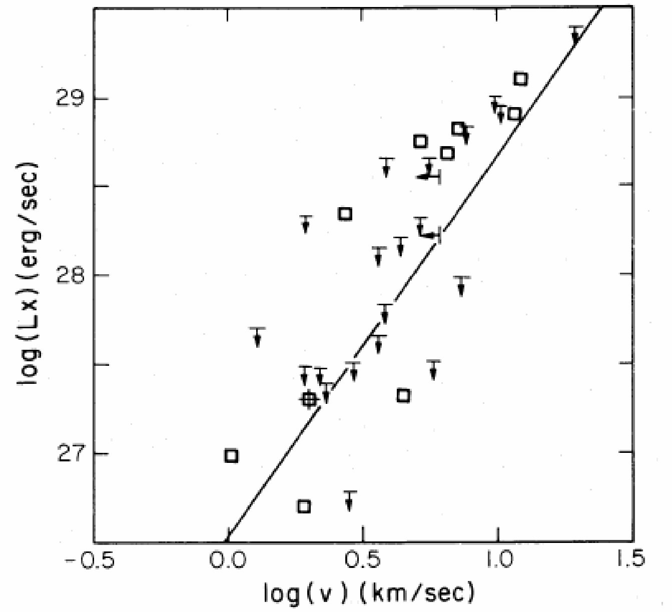

FIG. 7.—Scatter plot of X-ray luminosity vs. rotational velocity. Square, single stars. The indicated best-fit power-law relation again assumes that all the multiple stars (detected or not) are upper limits.

Maggio et al 1987, *ApJ*, 315, 687

No L_x – *v*sin*i* correlation in O stars

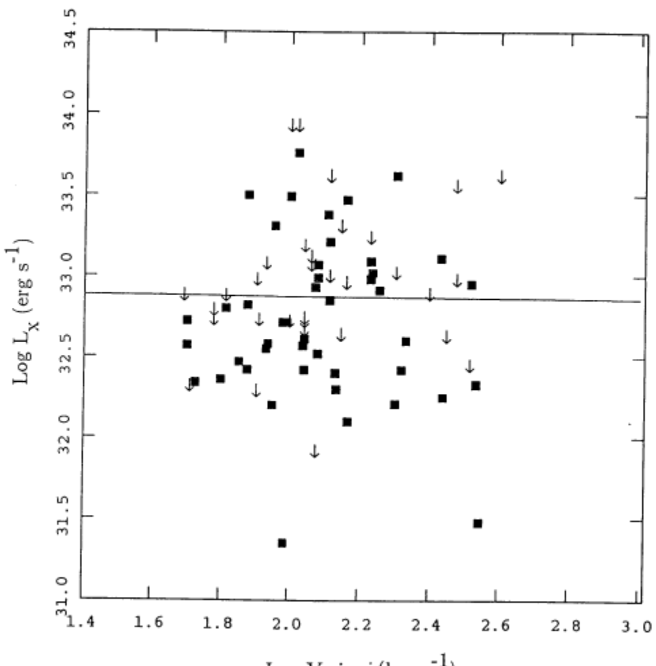

FIG. 16*f*

Sciortino et al. 1990, *ApJ*, 361, 621

Note higher L_x values for O stars; $L_x \sim 10^{-7}\ L_{Bol}$

Low-resolution X-ray observations: not enough attenuation of soft X-rays by the overlying wind to accommodate a corona

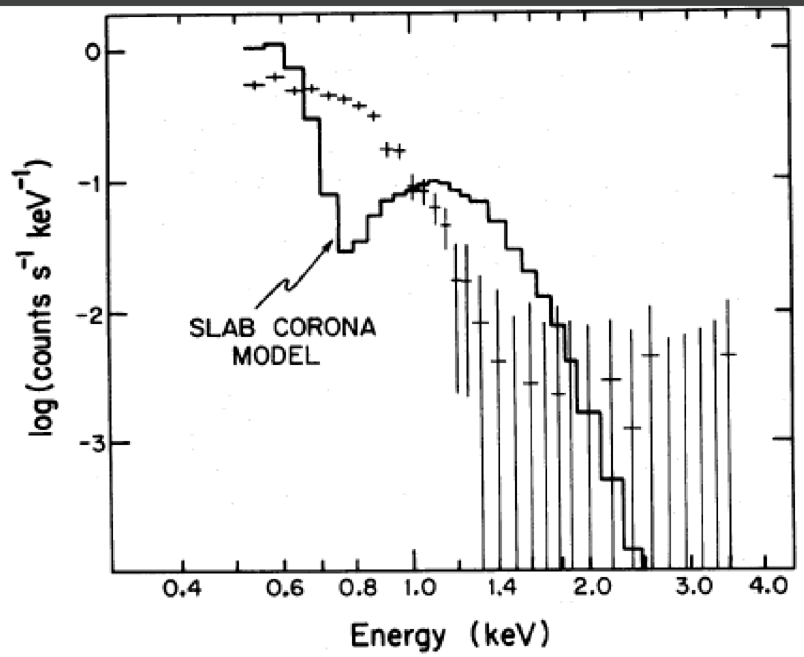

FIG. 3.—Shows a comparison of the SSS spectrum for ε Ori with the prediction of the slab corona plus cool wind model of Cassinelli and Olson (1979). The large absorption edge at 0.6 keV is caused by K shell ionization of oxygen occurring in the thick wind. The model shown corresponds to source parameters: $T = 1.7 \times 10^6$ K, $N_H = 10^{22.44}$ cm^{-2}, EM $= 10^{58}$ cm^{-3}.

Cassinelli & Swank 1983, ApJ, 241, 681

Mon. Not. R. Astron. Soc. 000, 1–6 (2006) Printed 12 April 2006 (MN LaTeX style file v2.2)

Discovery of magnetic fields in the β Cephei star ξ^1 CMa and in several Slowly Pulsating B stars*

S. Hubrig[1]†, M. Briquet[2]‡, M. Schöller[1], P. De Cat[3], G. Mathys[1], and C. Aerts[2]
[1]European Southern Observatory, Casilla 19001, Santiago, Chile
[2]Instituut voor Sterrenkunde, Katholieke Universiteit Leuven, Celestijnenlaan 200B, B-3001 Leuven,
[3]Koninklijke Sterrenwacht van België, Ringlaan 3, B-1180 Brussel, Belgium

2006

The surprising magnetic topology of τ Sco: fossil remnant or dynamo output?*

J.-F. Donati[1]†, I.D. Howarth[2], M.M. Jardine[3], P. Petit[1], C. Catala[4], J.D. Landstreet[5], J.-C. Bouret[6], E. Alecian[4], J.R. Barnes[3] and T. Forveille[7]
[1] LATT, Observatoire Midi-Pyrénées, 14 Av. E. Belin, F–31400 Toulouse, France
[2] Department of Physics and Astronomy, University College London, Gower Street, London WC1E6BT, UK
[3] School of Physics and Astronomy, University of St Andrews, St Andrews, Scotland KY16 9SS, UK
[4] LESIA, CNRS–UMR 8109, Obs. de Paris, 5 Place Janssen, F–92195 Meudon Cedex, France
[5] Department of Physics and Astronomy, University of Western Ontario, London Ontario N6A3K7, Canada
[6] LAM, Observatoire de Marseille-Provence, Traverse du Siphon BP 8, F–13376 Marseille Cedex 12, France
[7] CFHT, 65-1238 Mamalahoa Hwy, Kamuela HI, 96743 USA

2006, MNRAS, submitted

The Astrophysical Journal, 637:506–517, 2006 January 20

WINDS FROM OB STARS: A TWO-COMPONENT SCENARIO?

D. J. Mullan
Department of Physics and Astronomy, University of Delaware, Newark, D
AND
W. L. Waldron
L-3 Communications Government Services, Inc., Largo, MD 20774-5370
Received 2005 July 21; accepted 2005 Septemb

Adobe Acrobat Professional - [mullan_macdonald.pdf]

Mon. Not. R. Astron. Soc. 356, 1139–1148 (2005) doi:10.1111/j.1365-2966.2004.08544.x

Dynamo-generated magnetic fields at the surface of a massive star

D. J. Mullan[1]★ and James MacDonald[2]★
[1]Bartol Research Institute, University of Delaware, Newark DE 19716, USA
[2]Department of Physics and Astronomy, University of Delaware, Newark DE 19716, USA

Accepted 2004 October 23. Received 2004 October 21; in original form 2004 March 29

ABSTRACT
Spruit has shown that an astrophysical dynamo can operate in the non-convective material
ting star as a result of a particular instability in the magnetic field (the
assuming that the dynamo operates in a state of marginal instability,
mulae which predict the equilibrium strengths of azimuthal and radial
rms of local physical quantities. Here, we apply Spruit's formulae to
ed models of rotating massive stars in order to estimate Tayler dynamo
are no free parameters in Spruit's formulae. In our models of 10- and
ro-age main sequence, we find internal azimuthal fields of up to 1 MG,
nponents of a few kG. Evolved models contain weaker fields. In order
he field strength at the stellar surface, we examine the conditions under
mo fields are subject to magnetic buoyancy. We find that conditions for
lap with those for buoyancy at intermediate to high magnetic latitudes.
ds emerge at the surface of a massive star between magnetic latitudes
oles. We attempt to estimate the strength of the field which emerges at
e star. Although these estimates are very rough, we find that the surface
with values which have been reported recently for line-of-sight fields
in several O and B stars.

Key words: stars: early-type – stars: magnetic fields – stars: rotation.

1 of 10

The Astrophysical Journal, 586:480–494, 2003 March 20

MAGNETIC FIELDS IN MASSIVE STARS. II. THE BUOYANT RISE OF MAGNETIC FLUX TUBES THROUGH THE RADIATIVE INTERIOR

K. B. MacGregor[1] and J. P. Cassinelli[1,2]
Received 2001 November 8; accepted 2001 November 21

Radiation-driven winds of O and early-B stars

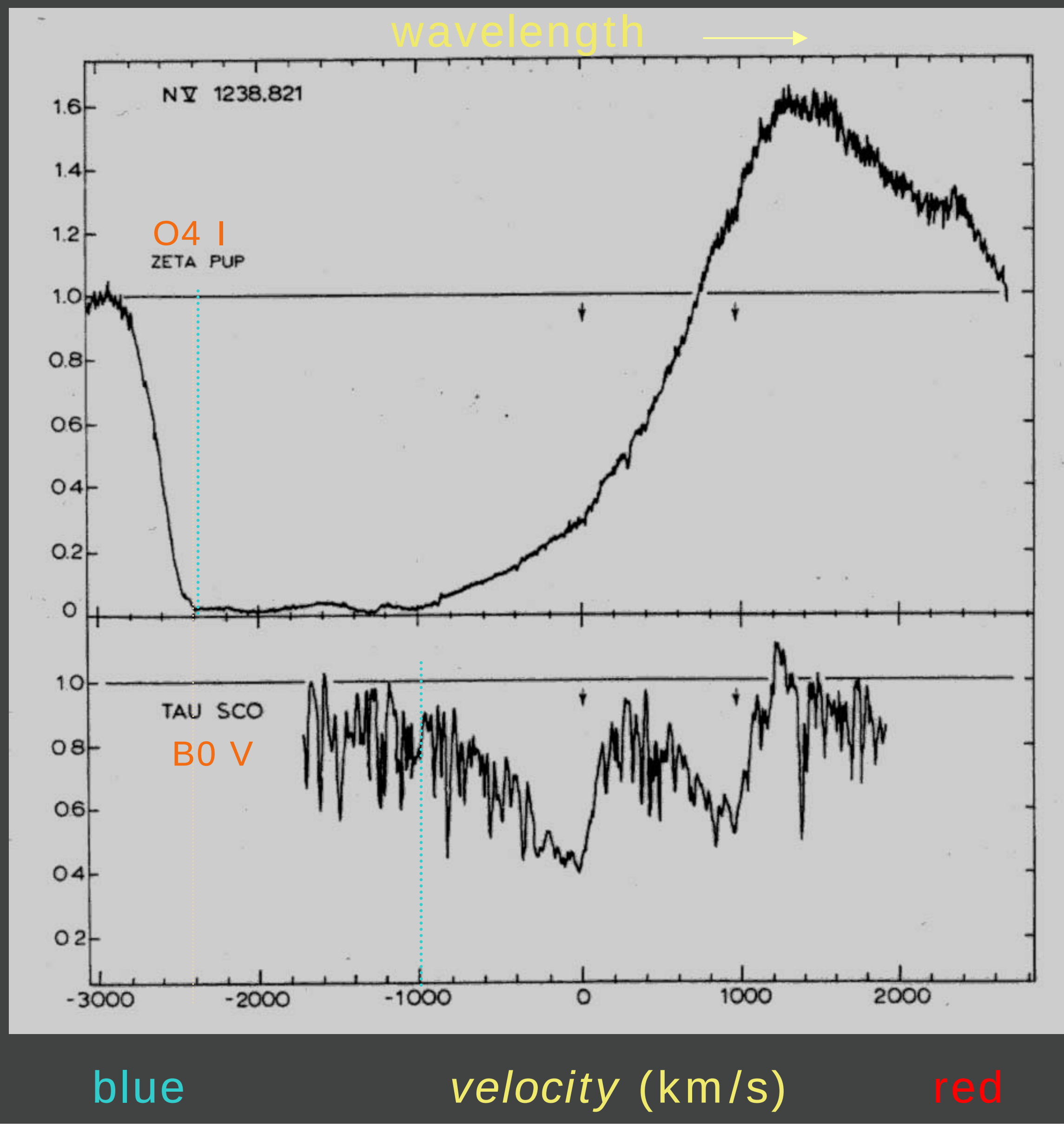

Line driving has an inherent instability

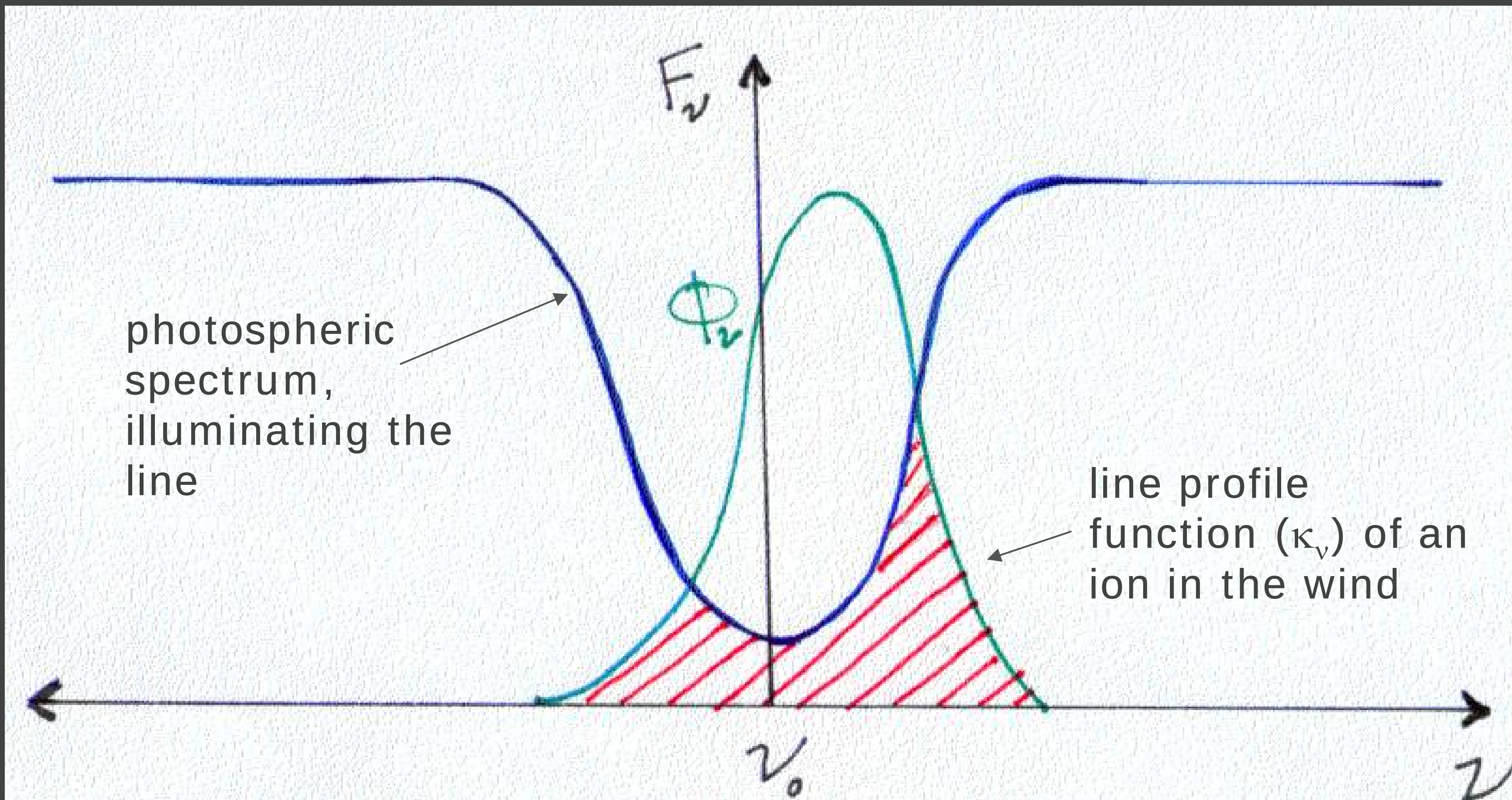

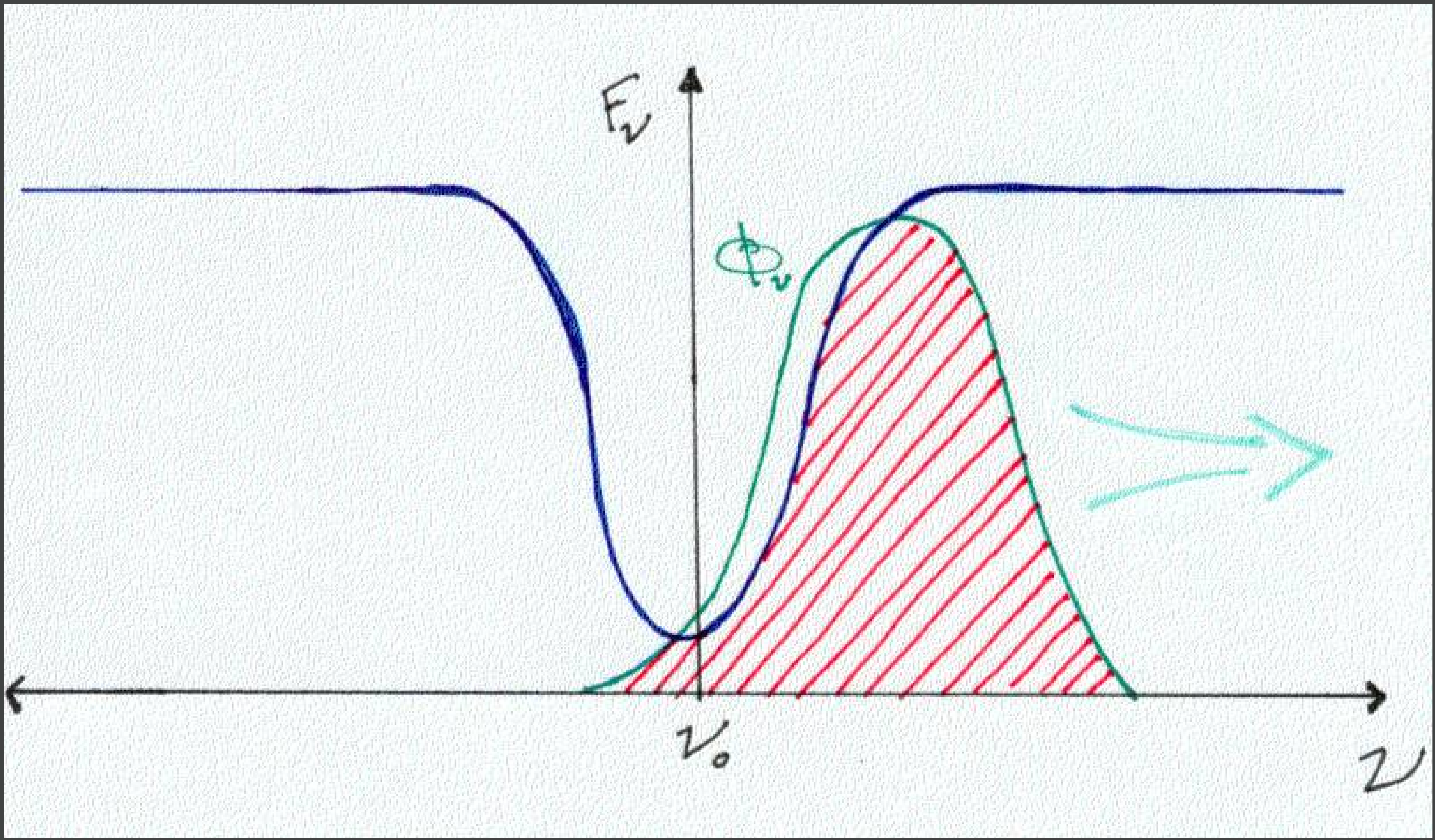

If the ion is perturbed, it moves out of the Doppler shadow, absorbs more radiation, and is further accelerated...

The line-driven instability (LDI) should lead to shock-heating and X-ray emission

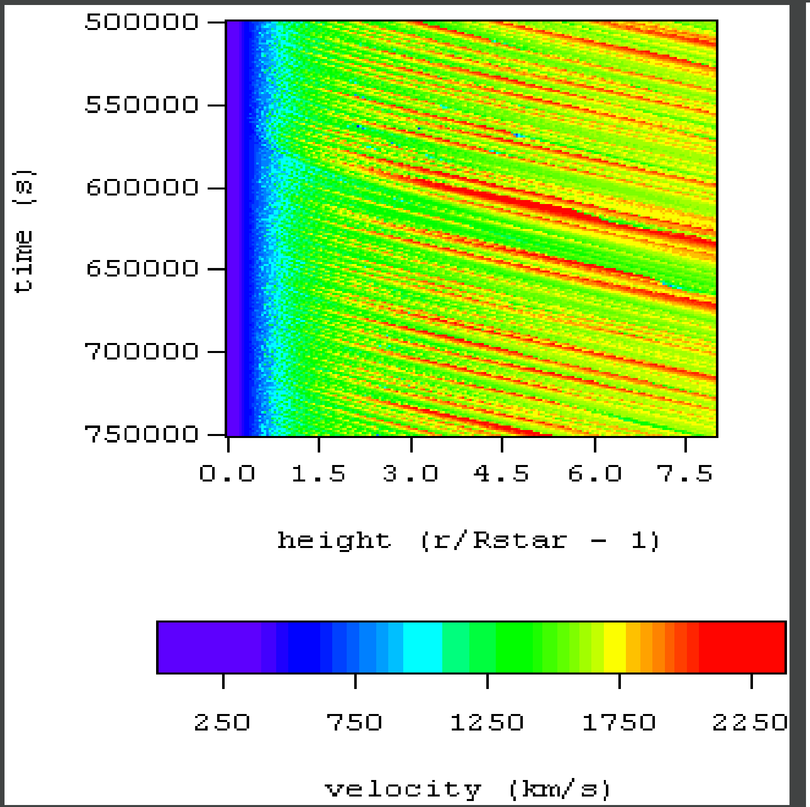

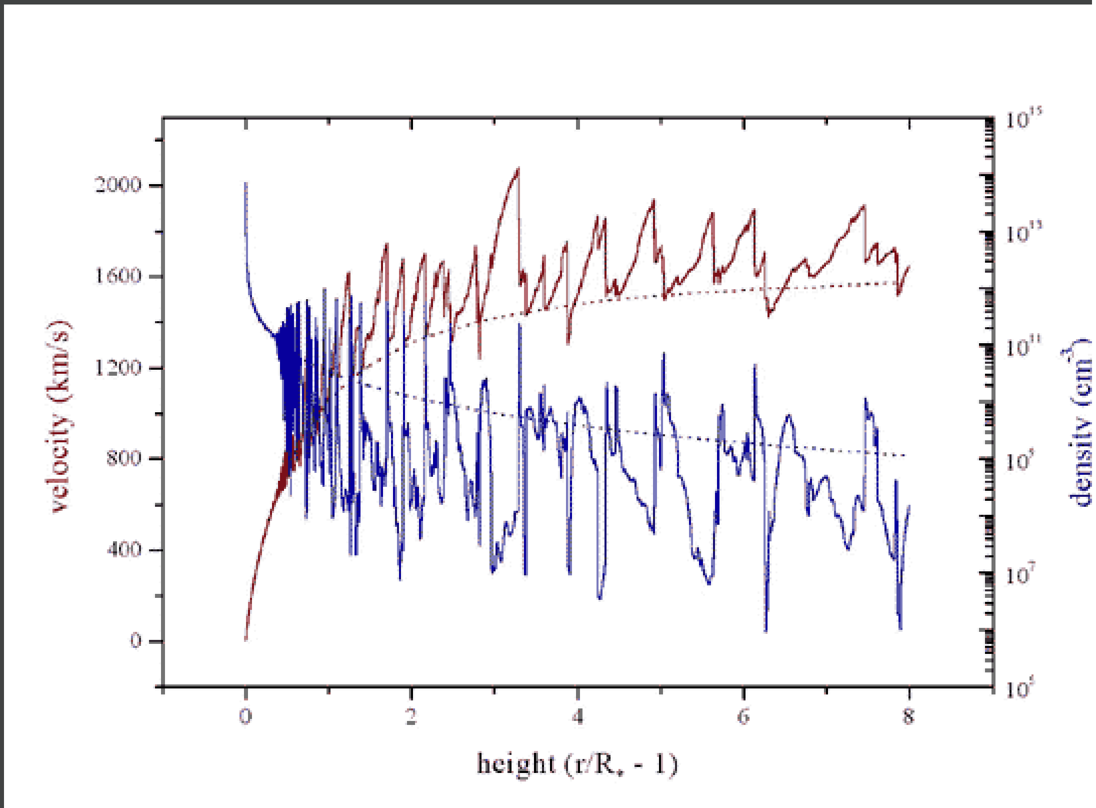

1-D rad-hydro simulation of the LDI

A snapshot at a single time from the same simulation.
Note the shock fronts.

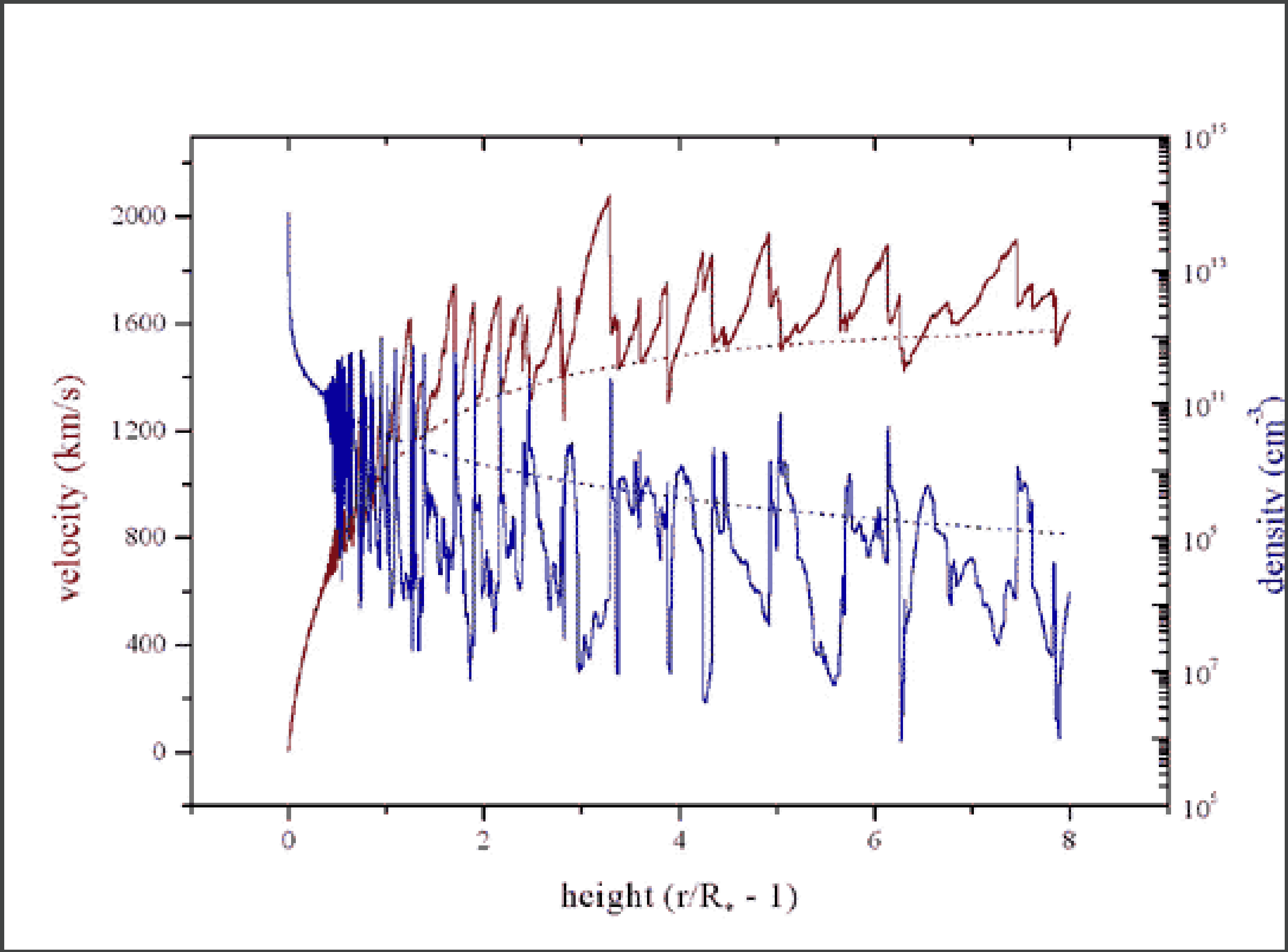

Most of the wind mass is in dense inter-shock regions, in which cold material provides a source of photoelectric absorption

Other groups find similar wind structure in their simulations

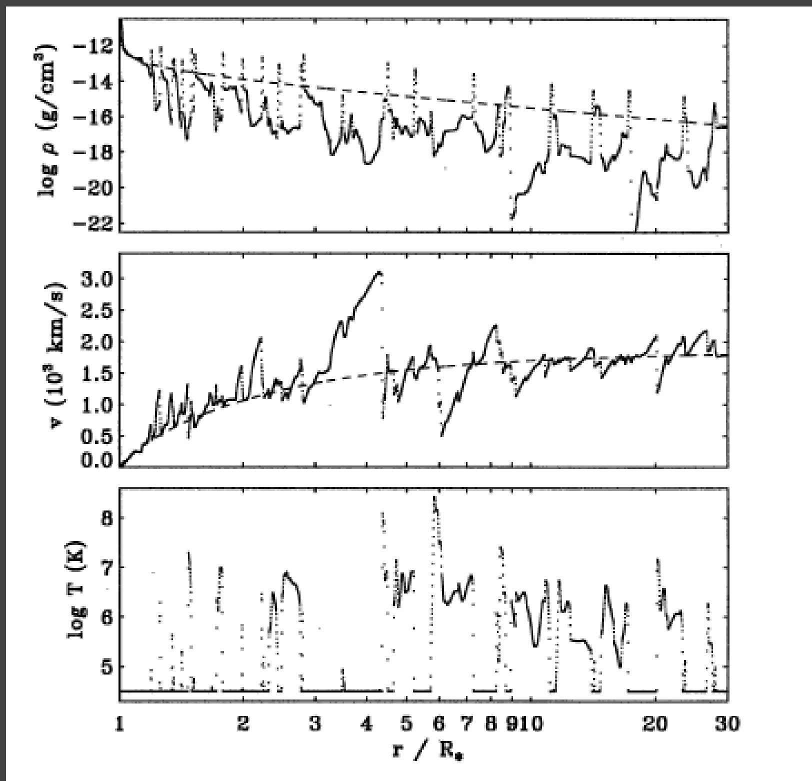

Fig. 13. Snapshot of the wind structure triggered by photospheric Langevin turbulence at three days after model start.

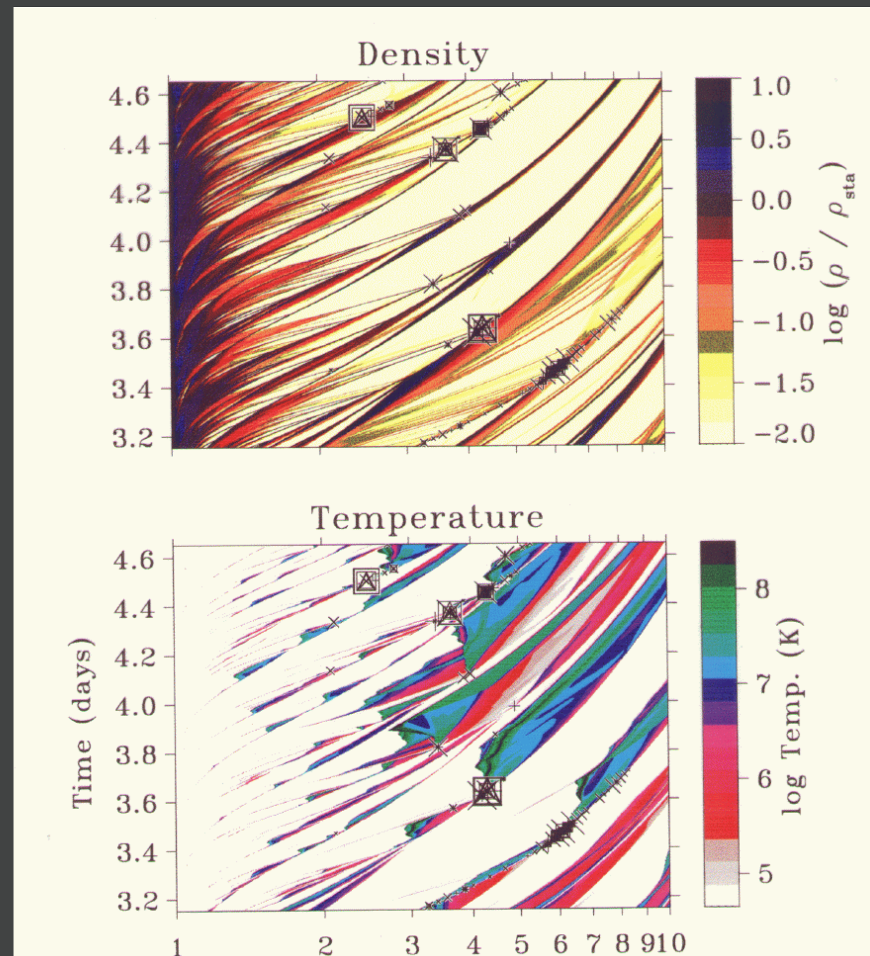

Feldmeier et al. 1997, *A&A*, 322, 878

There's ample evidence for wind variability and structure

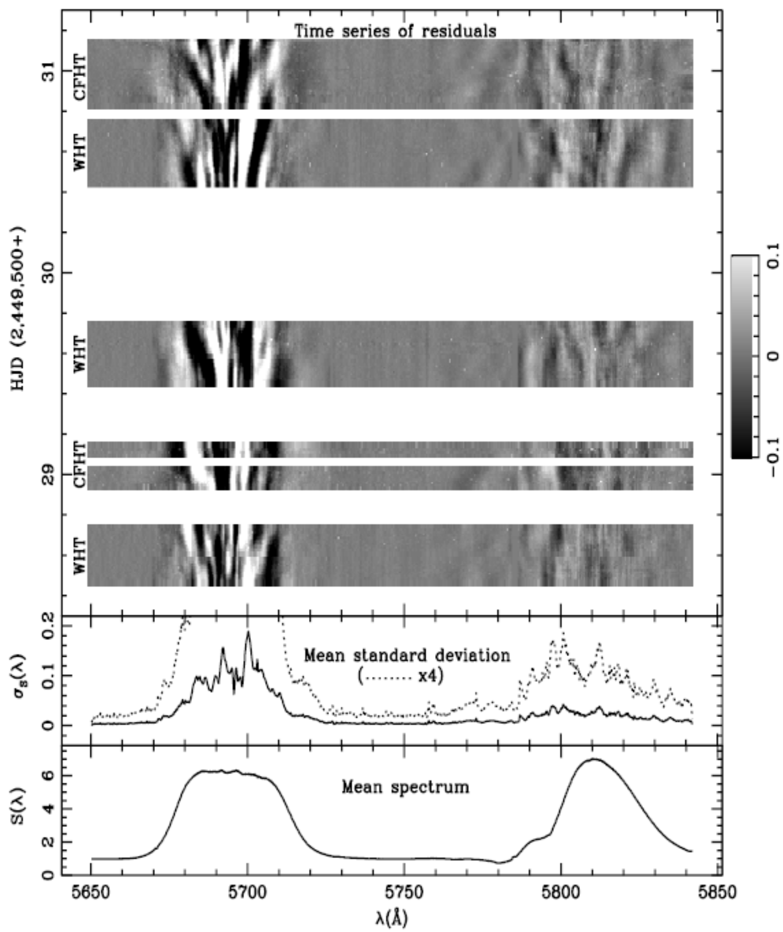

FIG. 2.—Combined CFHT and WHT spectroscopic monitoring of HD 192103. The mean profile for the whole data set is shown, along with the mean standard deviation, which indicates 4 times as much variability in the C III λ5696 emission line as in the C IV λ5808 doublet region. The gray-scale part is a time series of the residuals (obtained after subtracting off the global mean profile), detailing the variability pattern as a function of time. Note how the narrow emission features (*subpeaks*) appear to systematically move away from the line center. This pattern is consistent with the C III and C IV emission arising in a volume where the wind is clumped and accelerating away from the star.

Optical line profile variability in WR stars: from Lepine et al. 2000, *ApJ*, 120, 3201

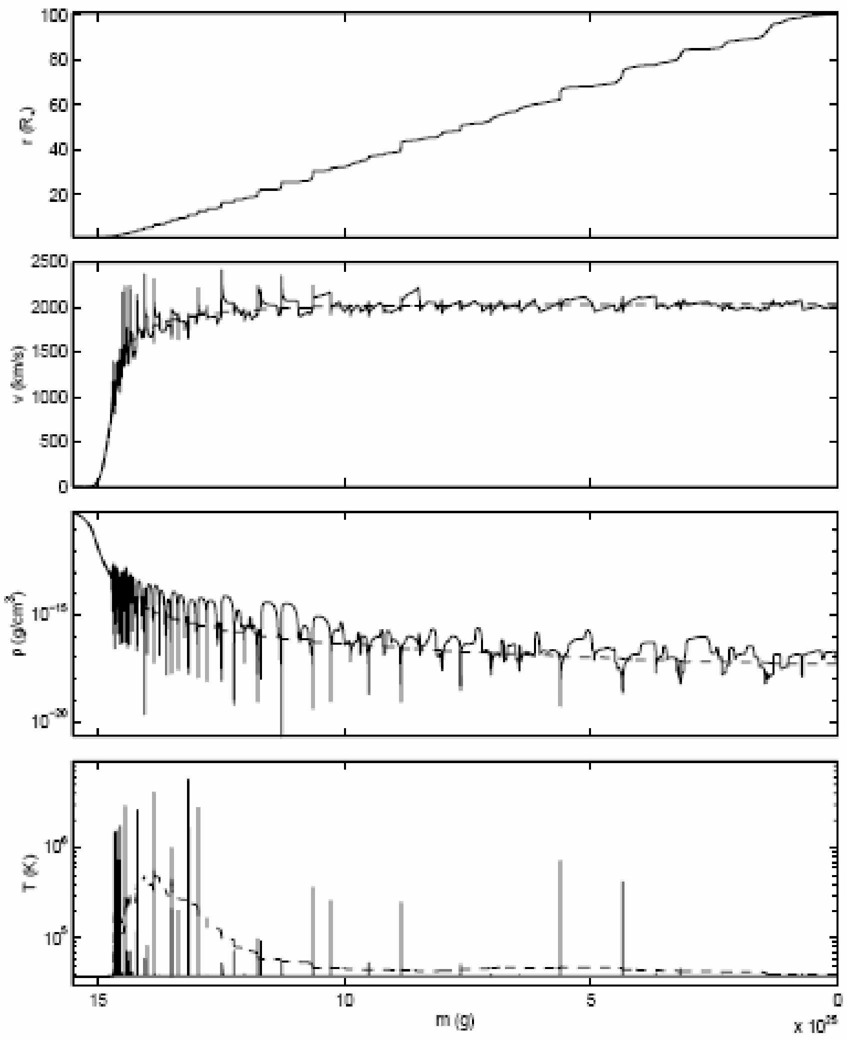

Fig. 4. Snapshot of the reference model at 2 Msec, now plotted versus the Lagrangian mass coordinate m defined in Eq. (10). The upper panel shows the Eulerian radius, while the remaining panels show the velocity, density, and temperature. The dashed lines in these lower panels show the corresponding time-averaged values.

Runacres & Owocki 2002, *A&A*, 381, 1015

Another rad-hydro simulation, but plotted in Lagrangian coordinates.

The shock-heated regions are a small fraction of the wind mass

Statistics from a long rad-hydro run (vs. radius)

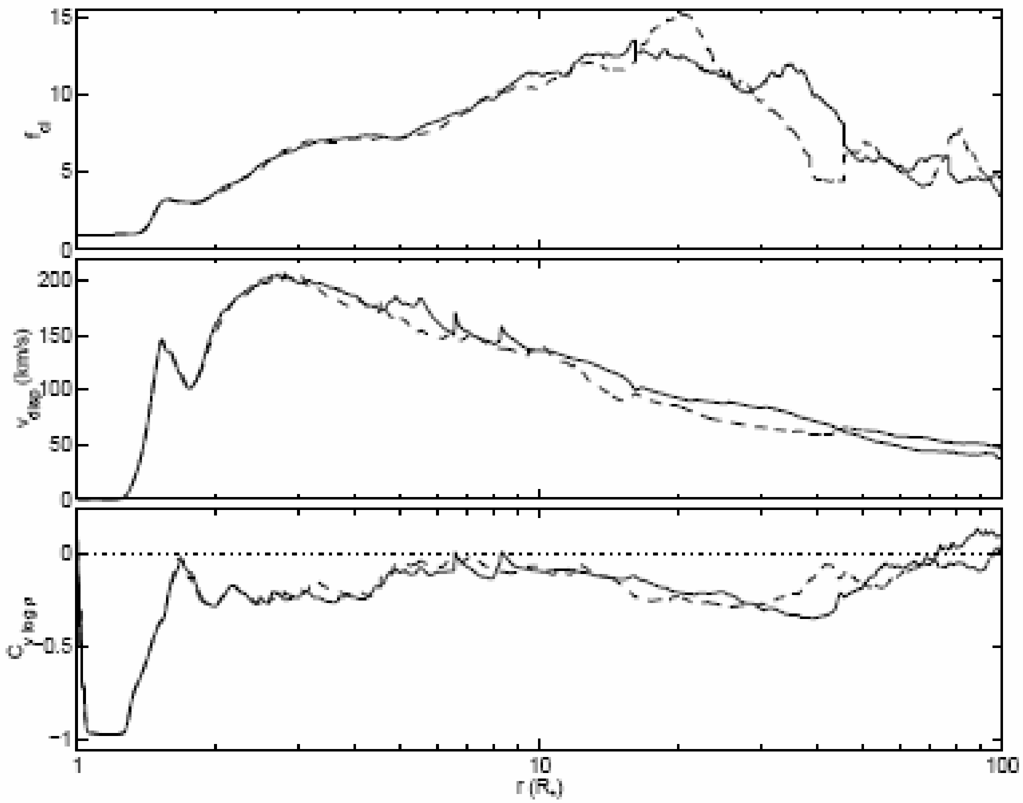

Fig. 5. Statistical properties of the reference model. The three panels, from top to bottom, show the clumping factor, the velocity dispersion, and the velocity-density correlation, all as a function of radius. The full line corresponds to averages taken between 2 and 2.5 Msec, the dashed line to averages taken between 2.5 and 3 Msec. The zero level for the correlation function is indicated by a dotted line.

clumping factor
$\rho_{clump}/\langle\rho\rangle$

velocity dispersion

density-velocity correlation

Runacres & Owocki 2002, *A&A*, 381, 1015

To analyze data, we need a simple, empirical model

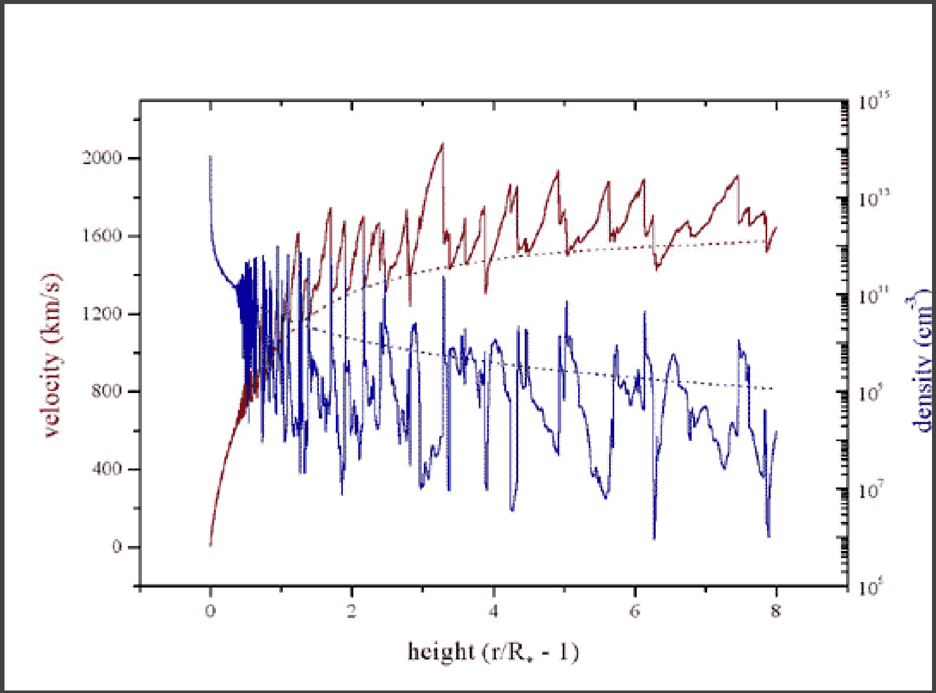

Detailed numerical model with lots of structure

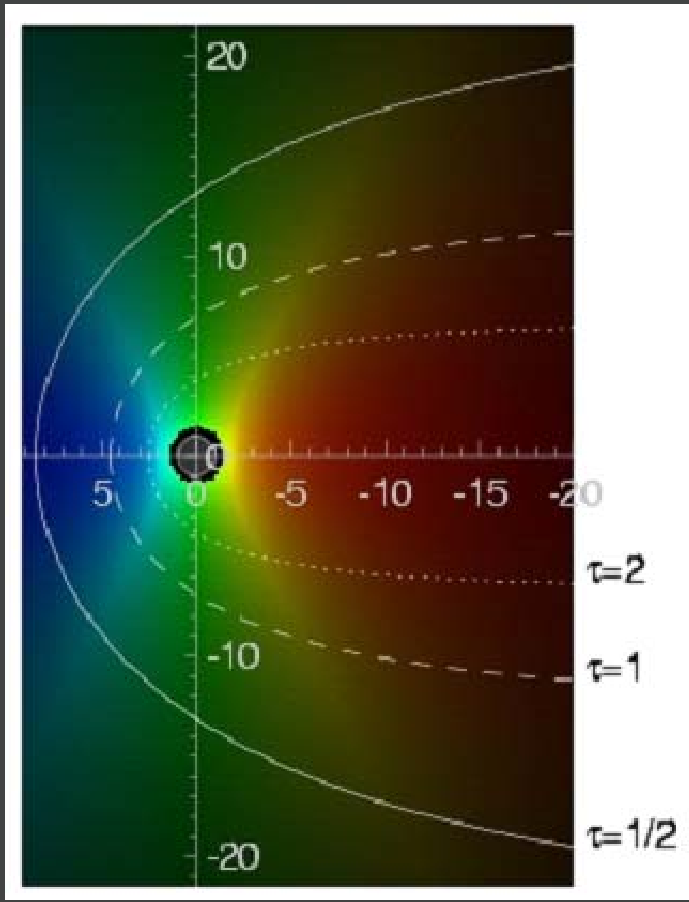

Smooth wind; two-component emission and absorption

Contours of constant optical depth
(observer is on the left)

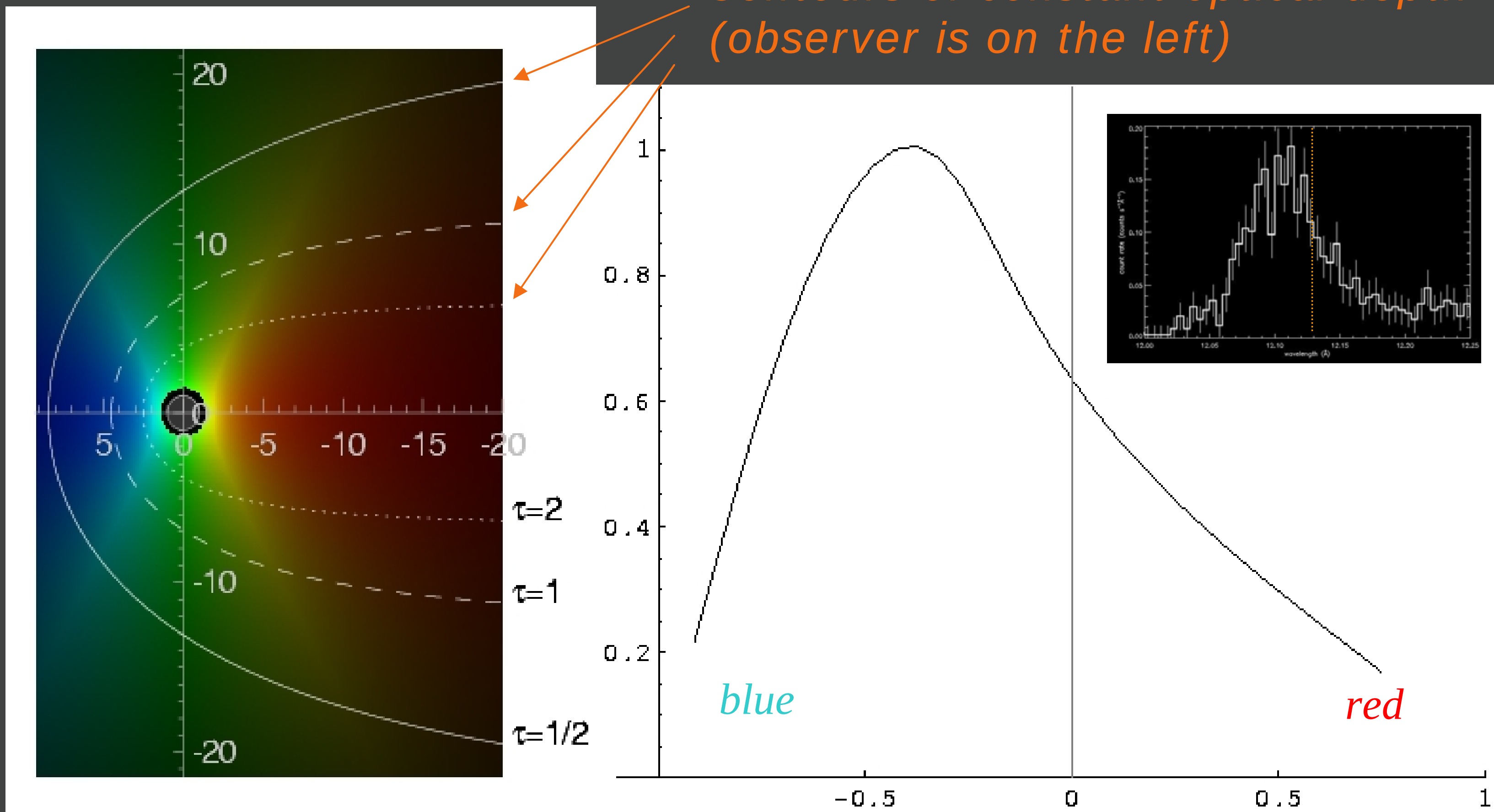

wavelength

continuum absorption in the bulk wind preferentially absorbs red shifted photons from the far side of the wind

The basic smooth wind model:

$$L_\lambda = 8\pi^2 \int_{-1}^{1} \int_{R_*}^{\infty} j e^{-\tau} r^2 dr d\mu$$

key parameters: $\mathbf{R_o}$ & τ_*

$j \propto \rho^2$ for $r/R_* > R_o$,

= 0 otherwise

$$\tau = \tau_* \int_z^{\infty} \frac{R_* dz'}{r'^2 (1 - R_*/r')^{\beta}}$$

$$\tau_* \equiv \frac{\kappa \dot{M}}{4 \pi R_* v_\infty}$$

τ_*=1,2,8

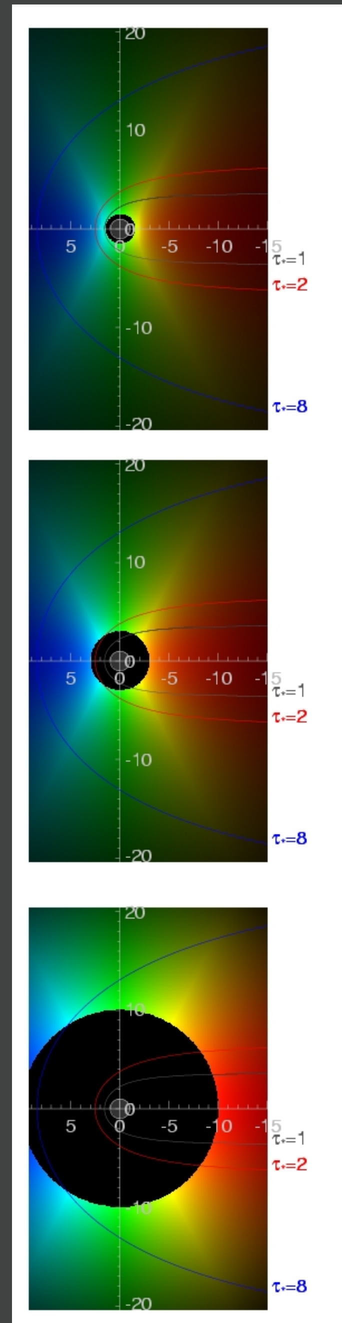

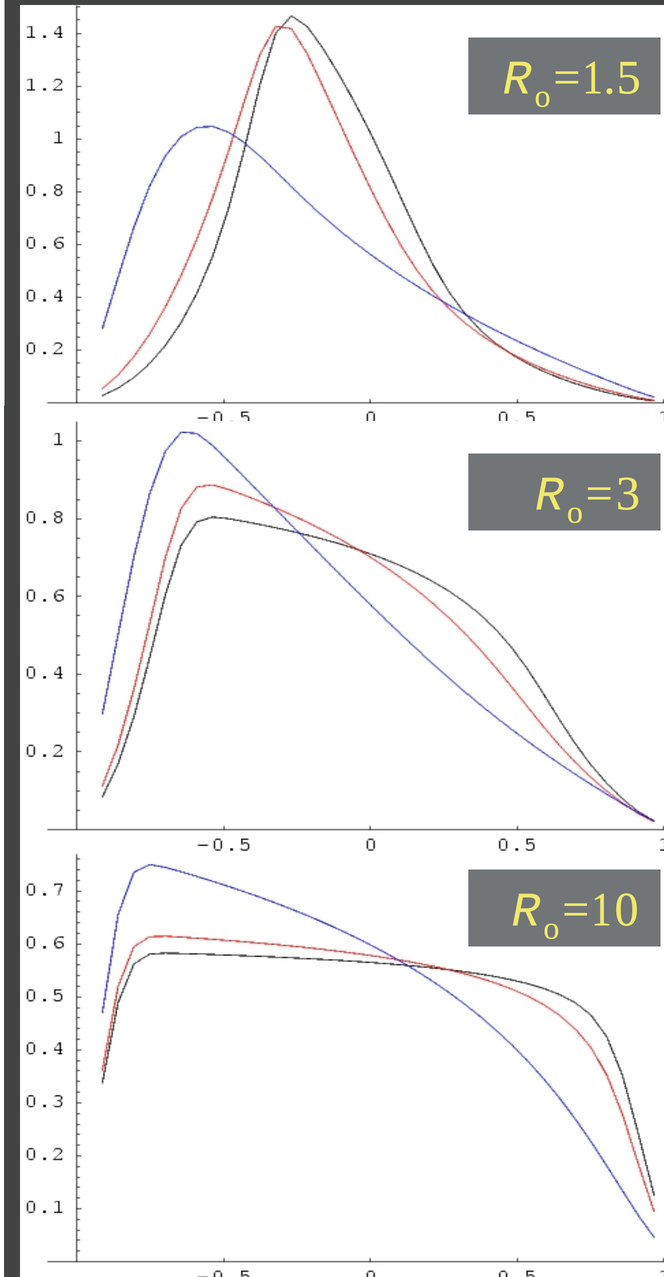

Highest S/N line in the ζ Pup *Chandra* spectrum

Fe XVII @ 15.014 Å

560 total counts

note Poisson error bars

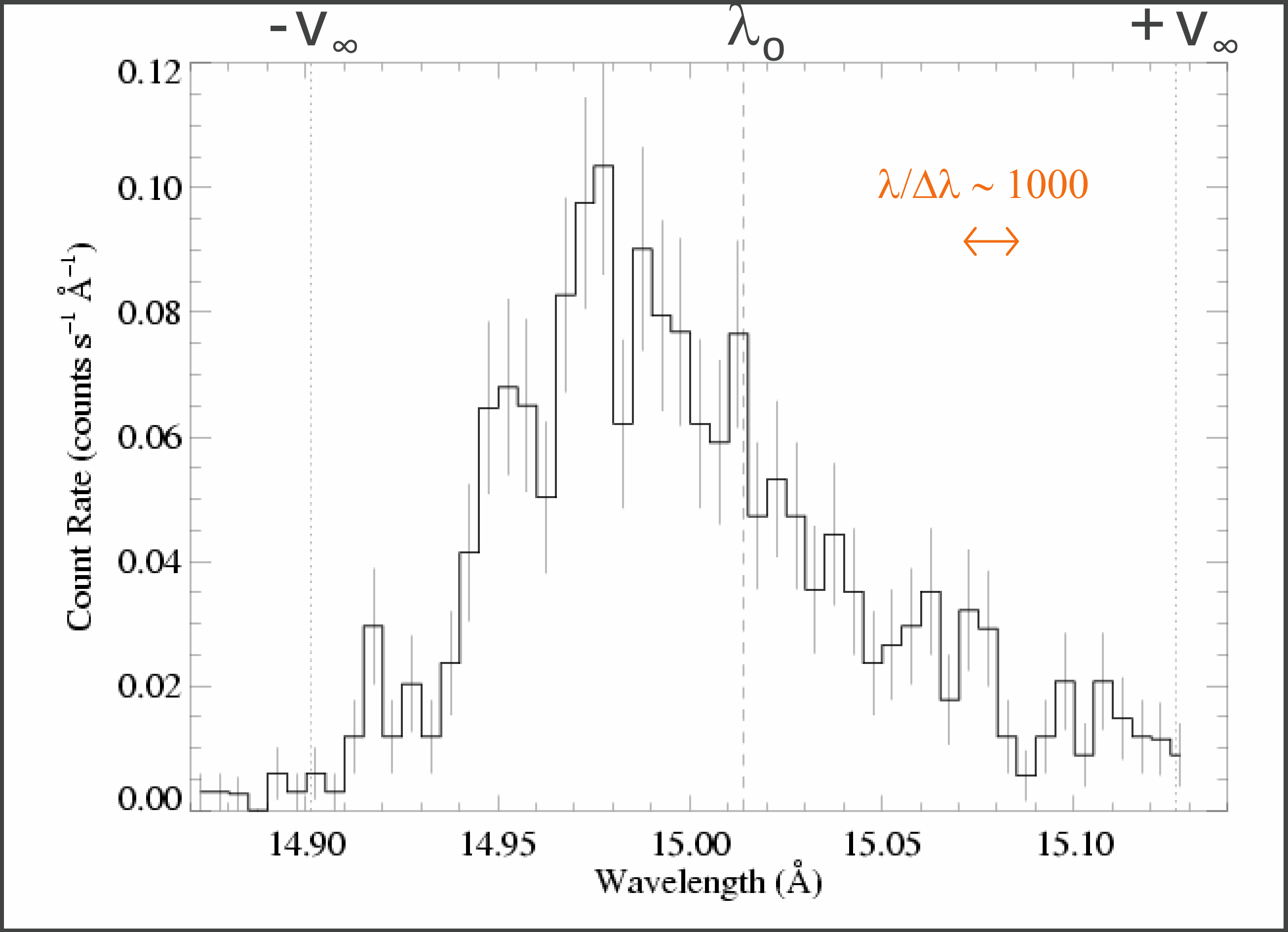

Fe^{+16} – neon-like; dominant stage of iron at $T \sim 3 \times 10^6$ K in this coronal plasma

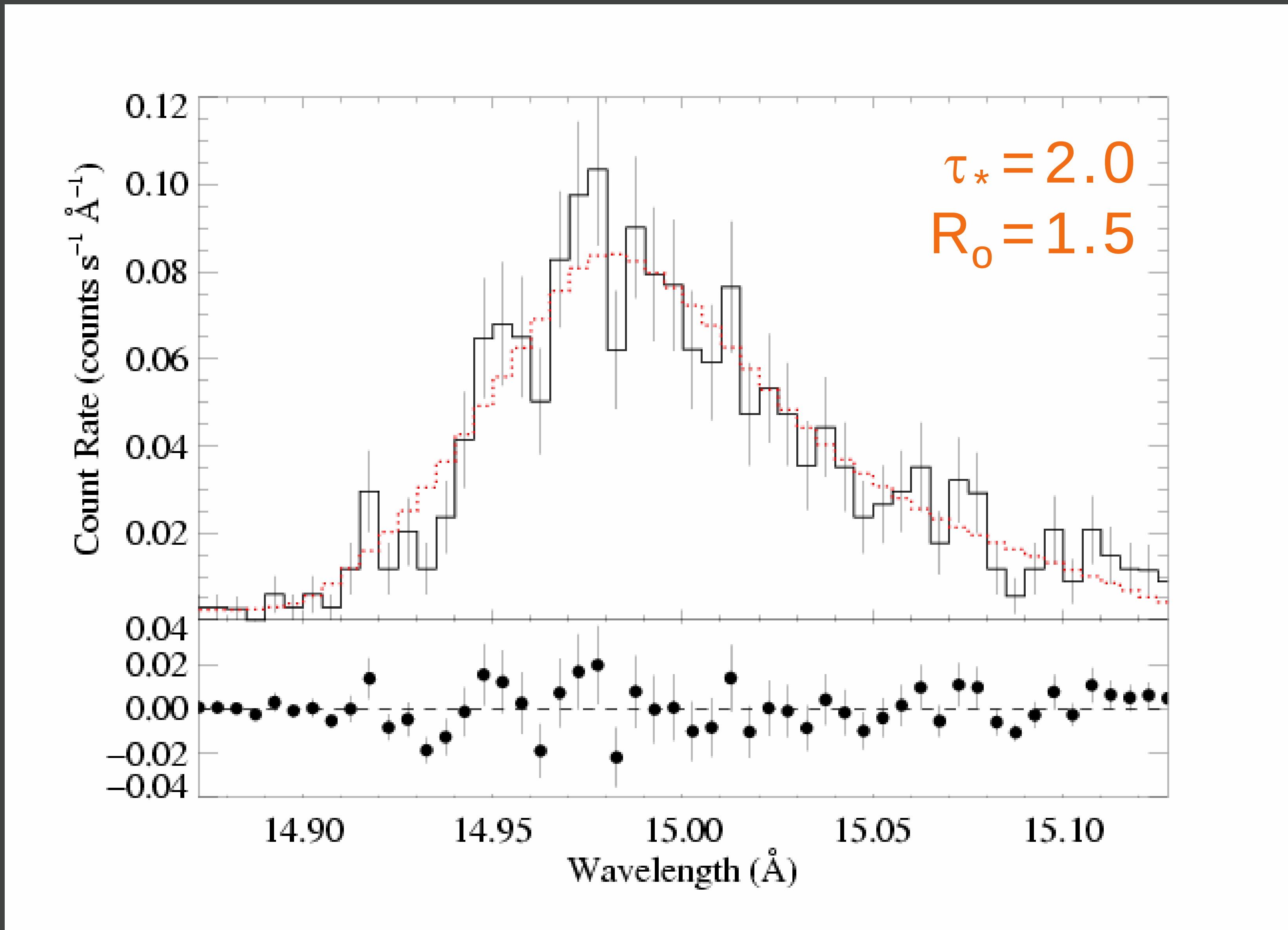

C = 98.5 for 103 degrees of freedom: *P* = 19%

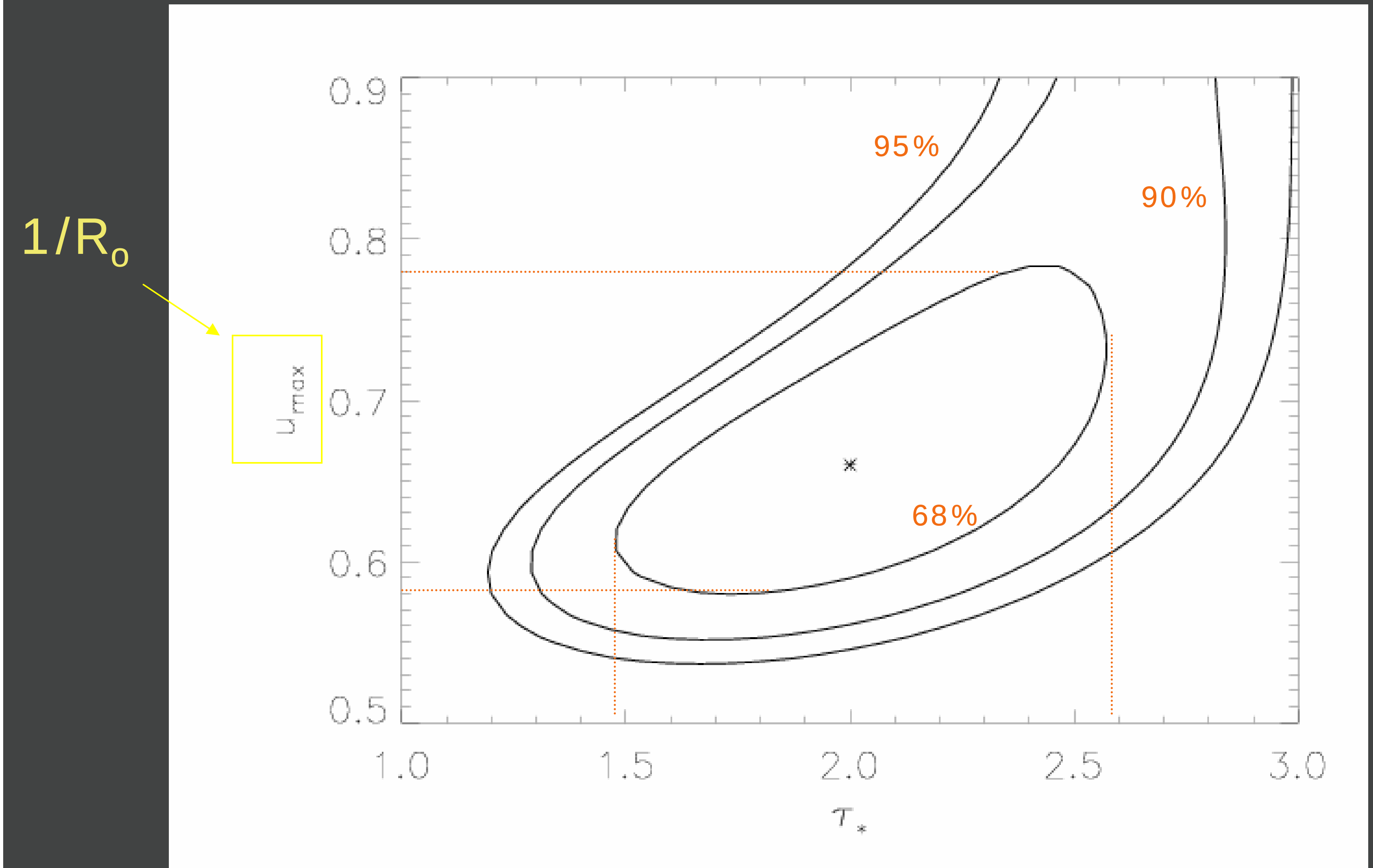

$1.5 < \tau_* < 2.6$ *and* $1.3 < R_o < 1.7$

Onset of shock-induced structure: $R_o \sim 1.5$

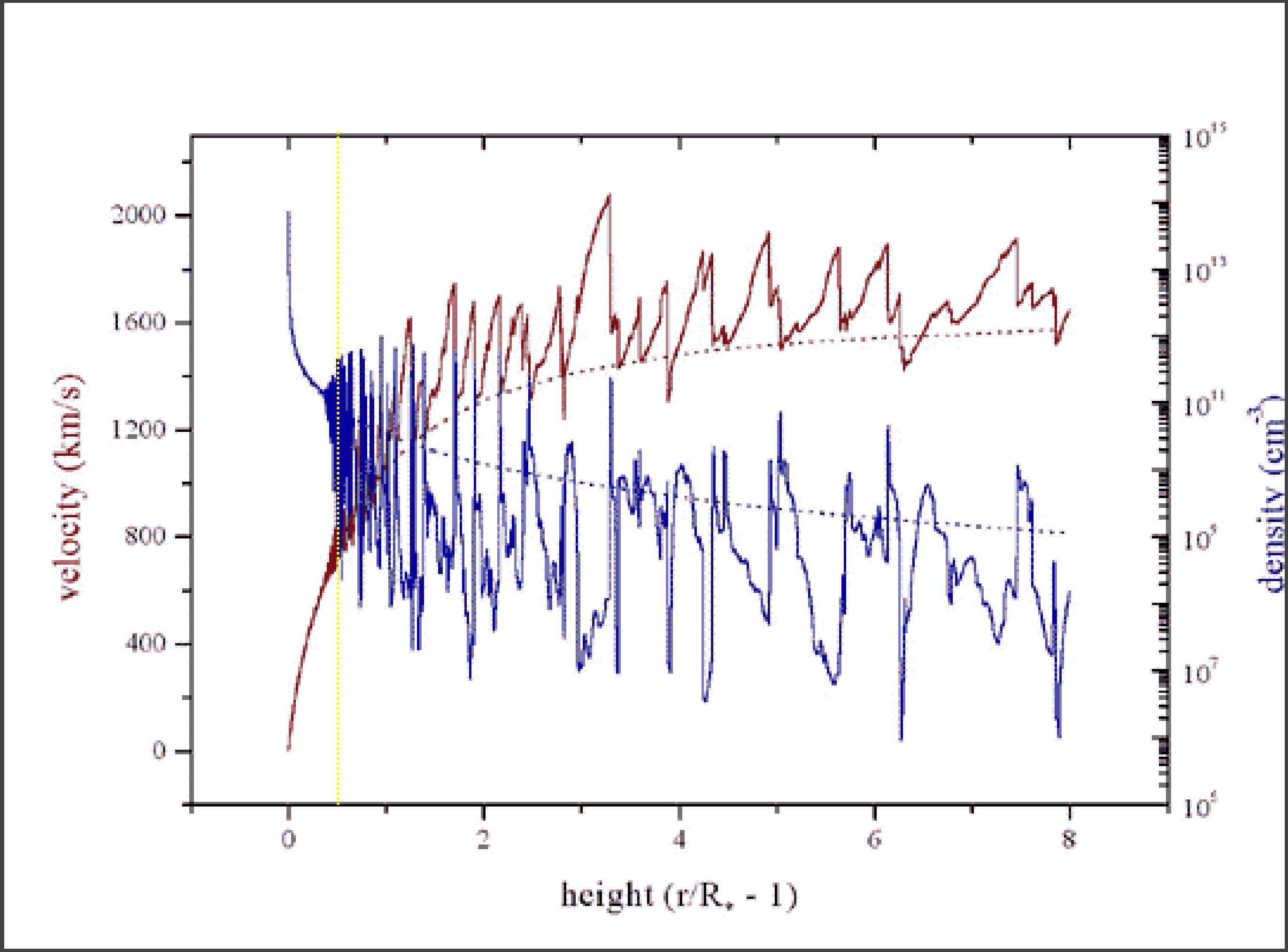

for $\tau_* = 2$

$$\tau_* \equiv \frac{\kappa \dot{M}}{4\pi R_* v_\infty}$$

$$\tau_* = \frac{3.6\kappa_{150}\dot{M}_{-6}}{R_{12}v_{2000}}$$

$$\dot{M}_{-6} = \frac{\tau_* R_{12} v_{2000}}{3.6\kappa_{150}}$$

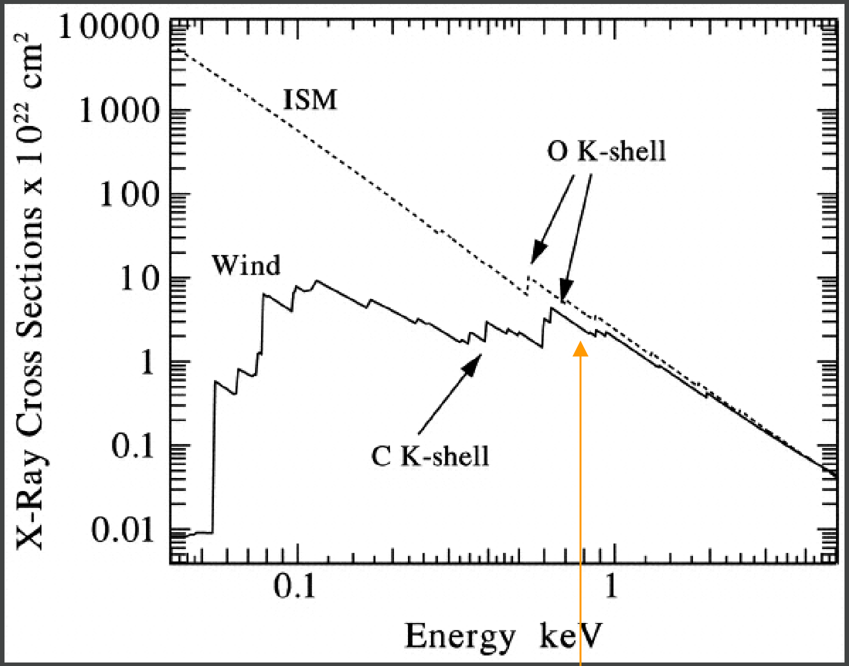

$\kappa \sim 150\ \mathrm{cm^2\ g^{-1}}$ @ 15 Å

$7 \times 10^{-7}\ M_{sun}/yr$

A **factor of 4** reduction in mass-loss rate over the literature value of $2.4 \times 10^{-6}\ M_{sun}/yr$

Best-fit smooth-wind model with $\tau_* = 8$

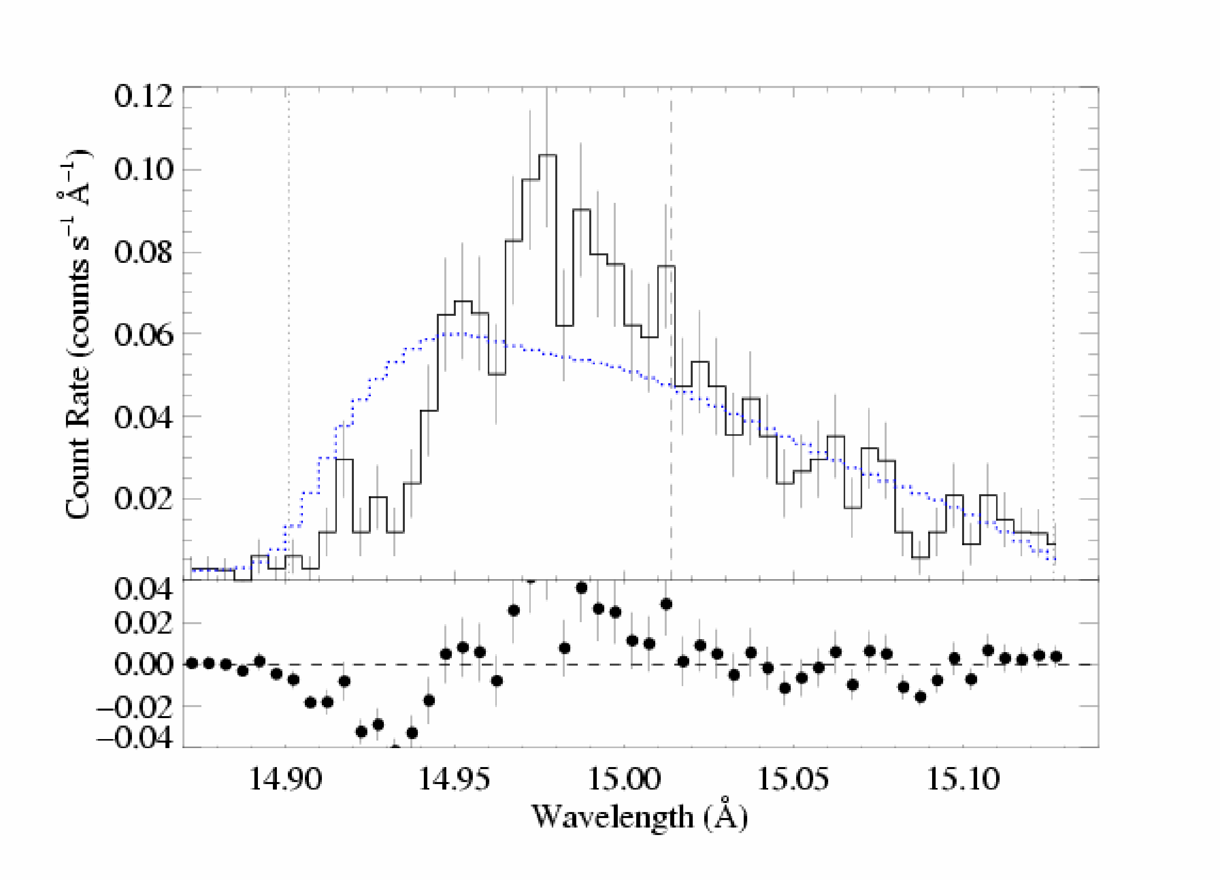

This is the value of τ_* expected from
$\dot{M}$ = 2.4 X 10^{-6} M_{sun}/yr

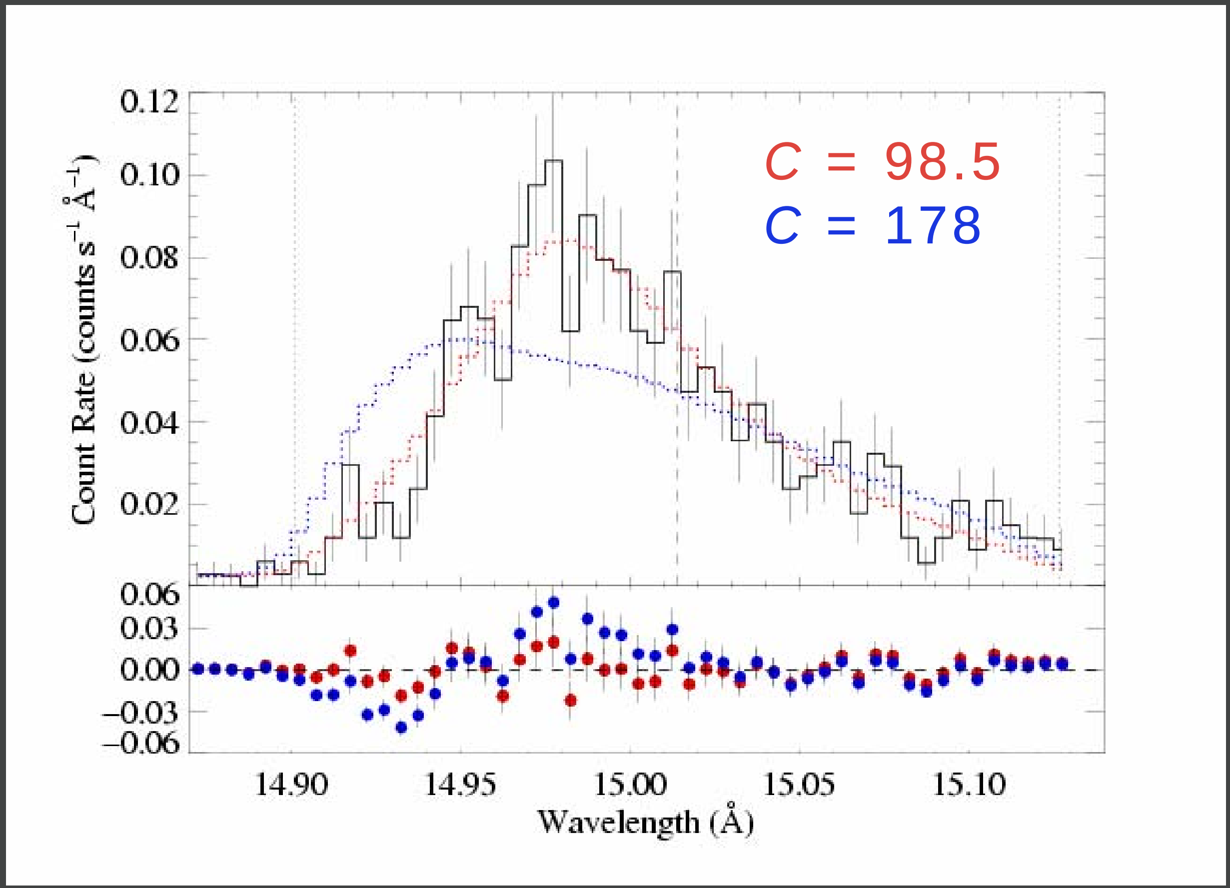

The best-fit model, with $\tau_* = 2$, is preferred over the $\tau_* = 8$ model with >99.999% confidence

The porosity associated with a distribution of optically thick clumps acts to reduce the effective opacity of the wind

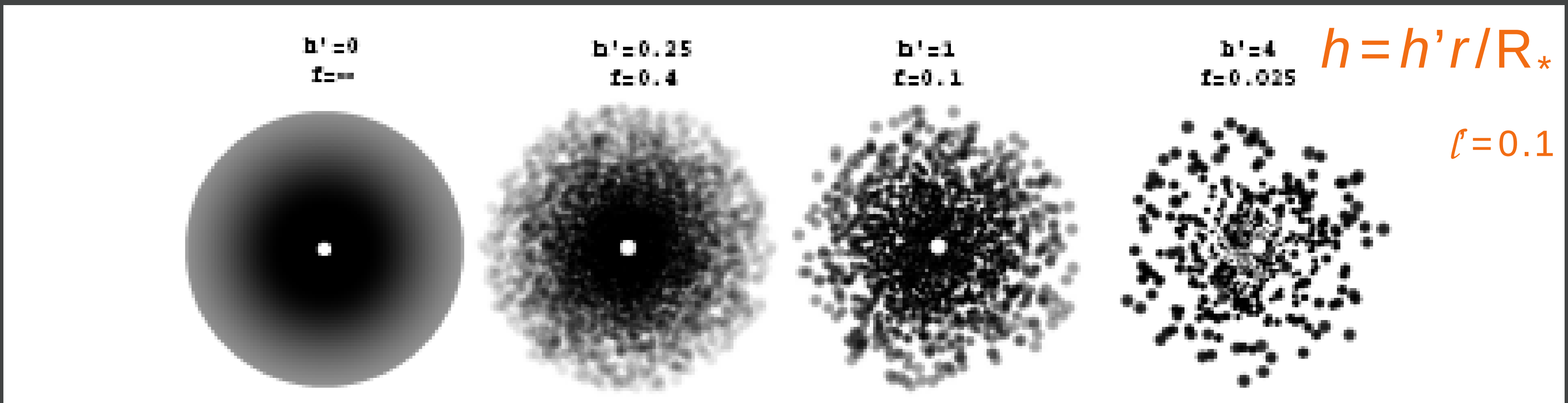

The key parameter is the **porosity length**,

$h = (L^3/\ell^2) = \ell/f$

Porosity reduces the effective wind optical depth once ***h*** becomes comparable to r/R_*

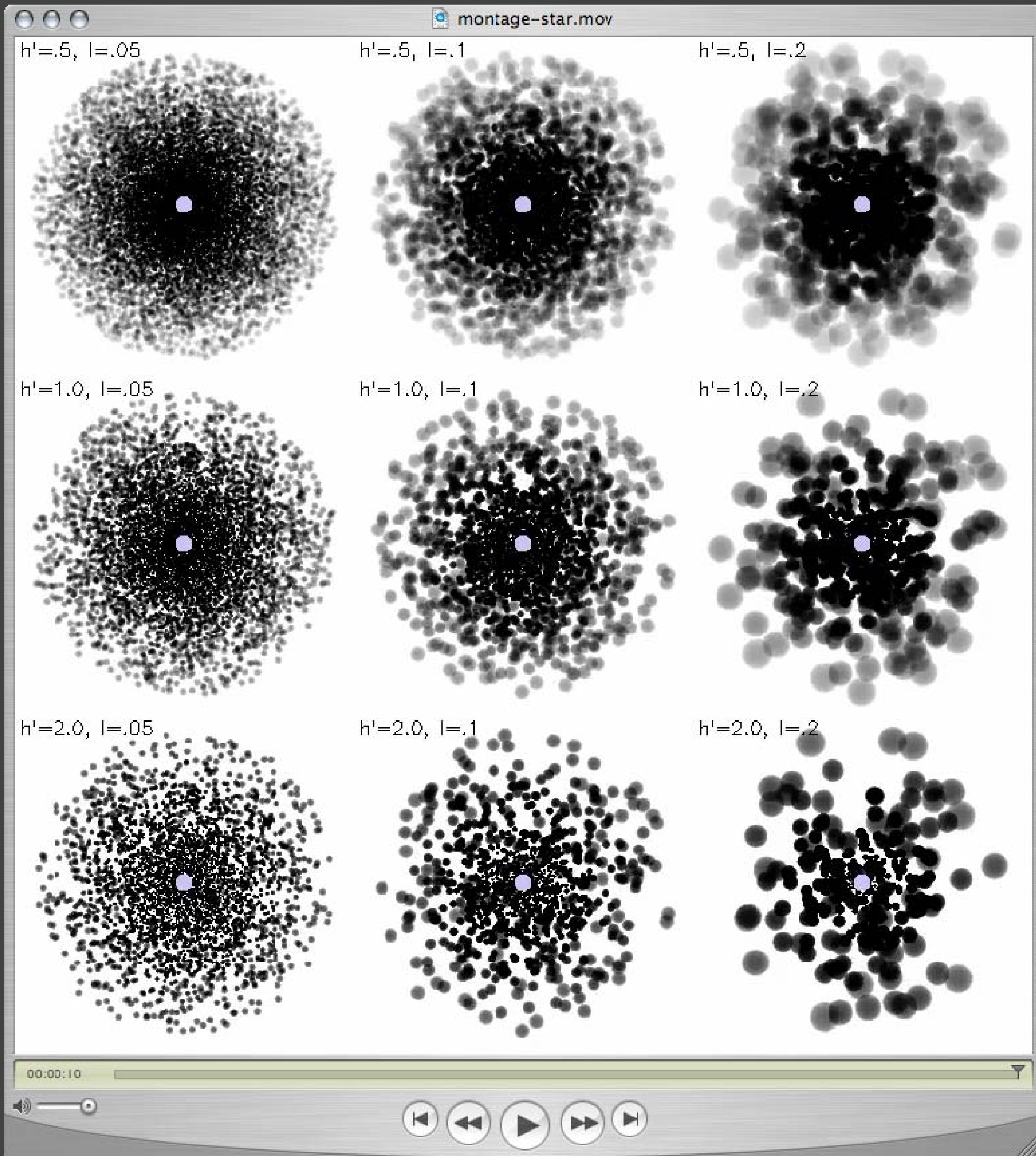

$$h = (L^3 / \ell^2) = \ell / f$$

The optical depth integral is modified according to the clumping-induced effective opacity:

$$\kappa_{eff} = \frac{\kappa\left(1 - e^{-\tau_c}\right)}{\tau_c}$$

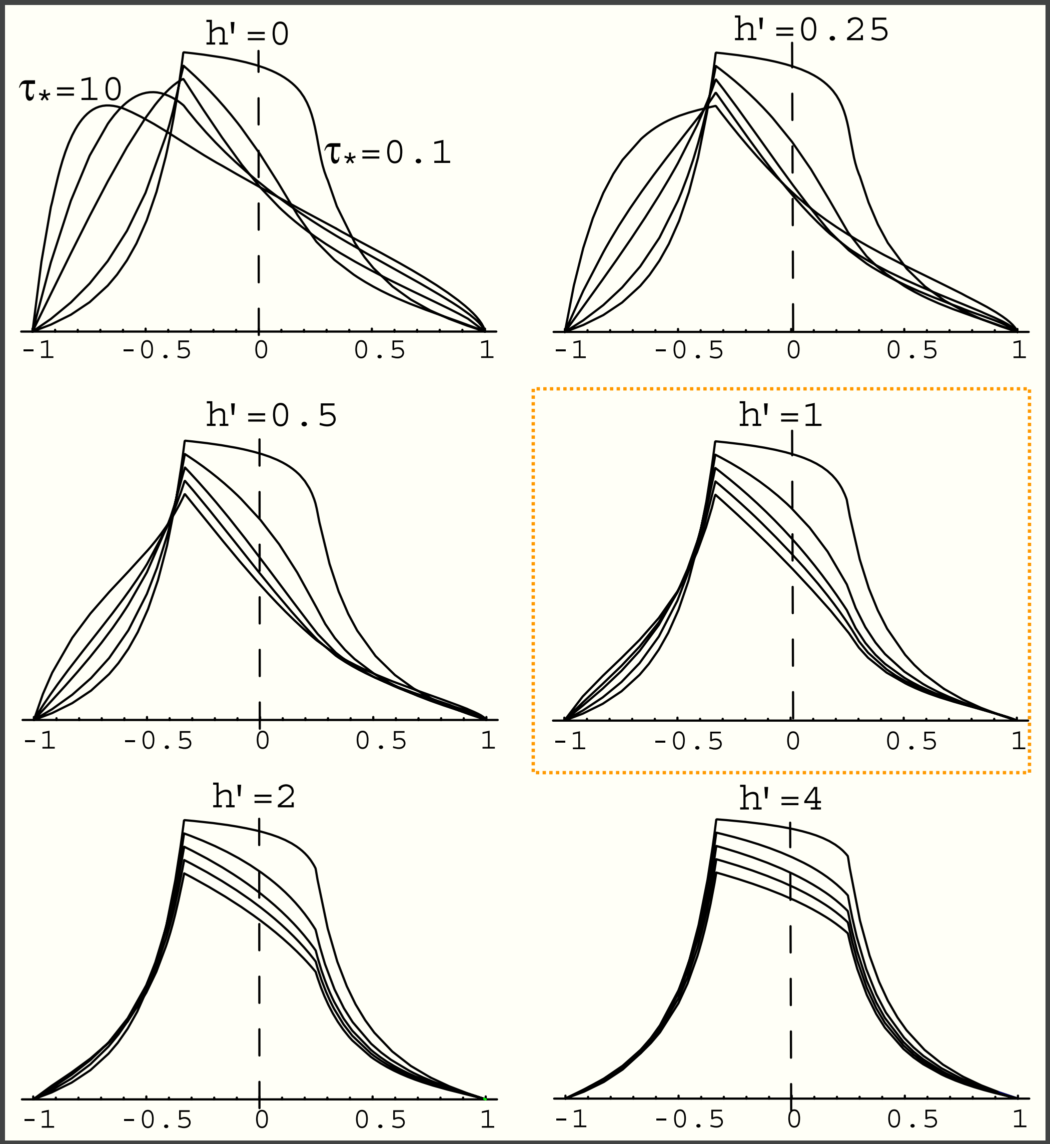

from Owocki & Cohen 2006, *ApJ*, 648, 565

Fitting models that include porosity from spherical clumps in a beta-law distribution: $h = h_\infty(1 - R_*/r)^\beta$

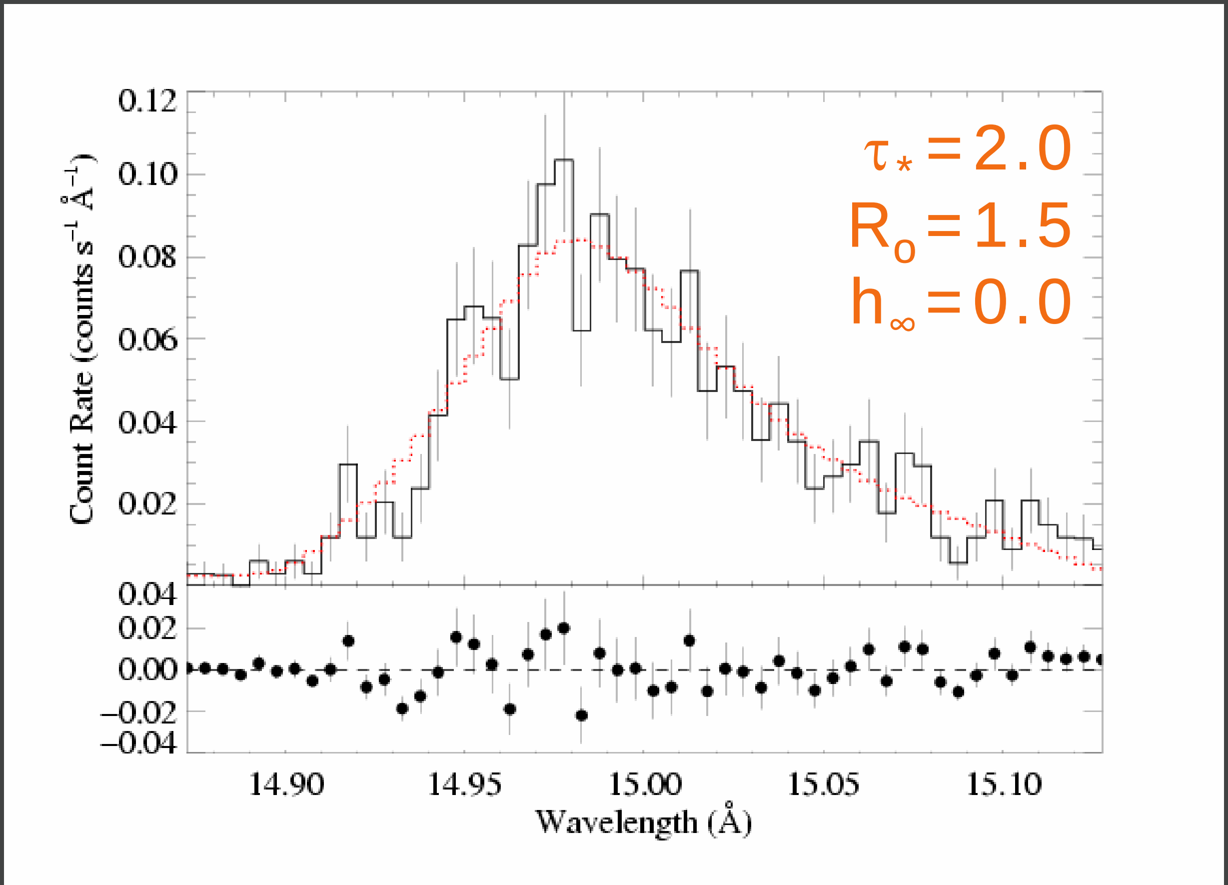

Identical to the smooth wind fit: $h_\infty = 0$ is the preferred value of h_∞.

Joint constraints on τ_* and h_∞

best-fit model with $\tau_*=8$

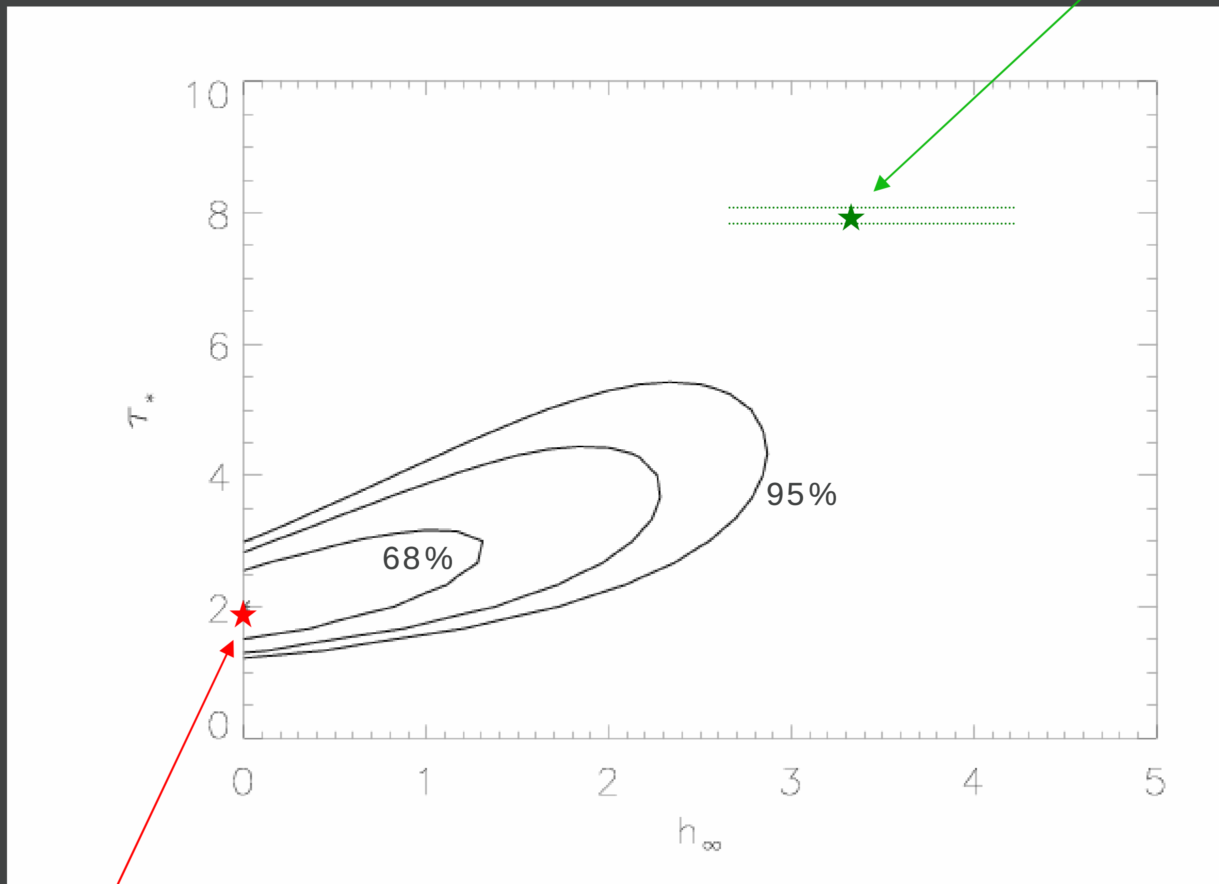

best-fit model

$\Delta C=9.4$: best-fit model is preferred over $\tau_*=8$ model with > 99% confidence

The differences between the models are subtle...

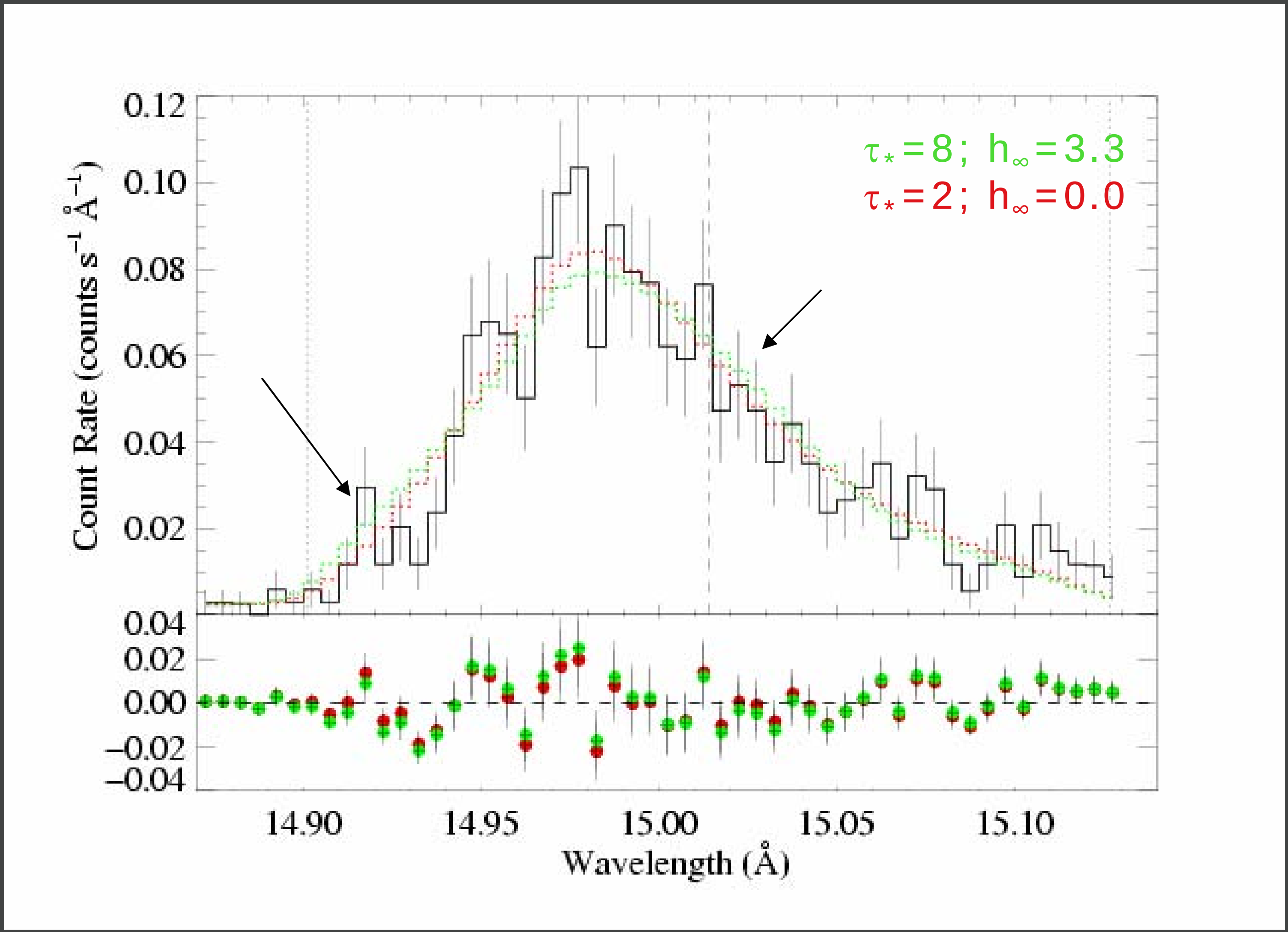

...but statistically significant

Two models from previous slide,
but with *perfect resolution*

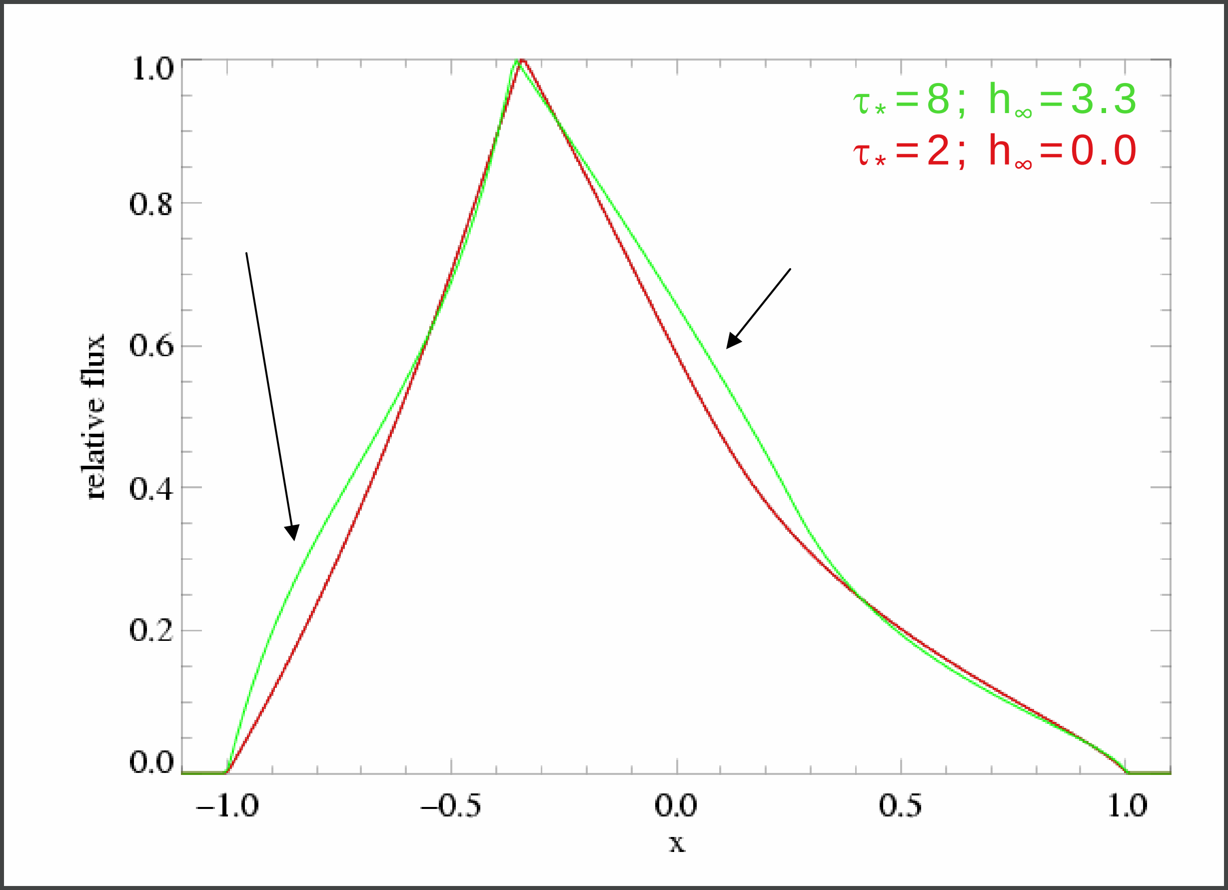

Joint constraints on τ_* and h_∞

$h_\infty > 2.5$ is required if you want to "rescue" the literature mass-loss rate

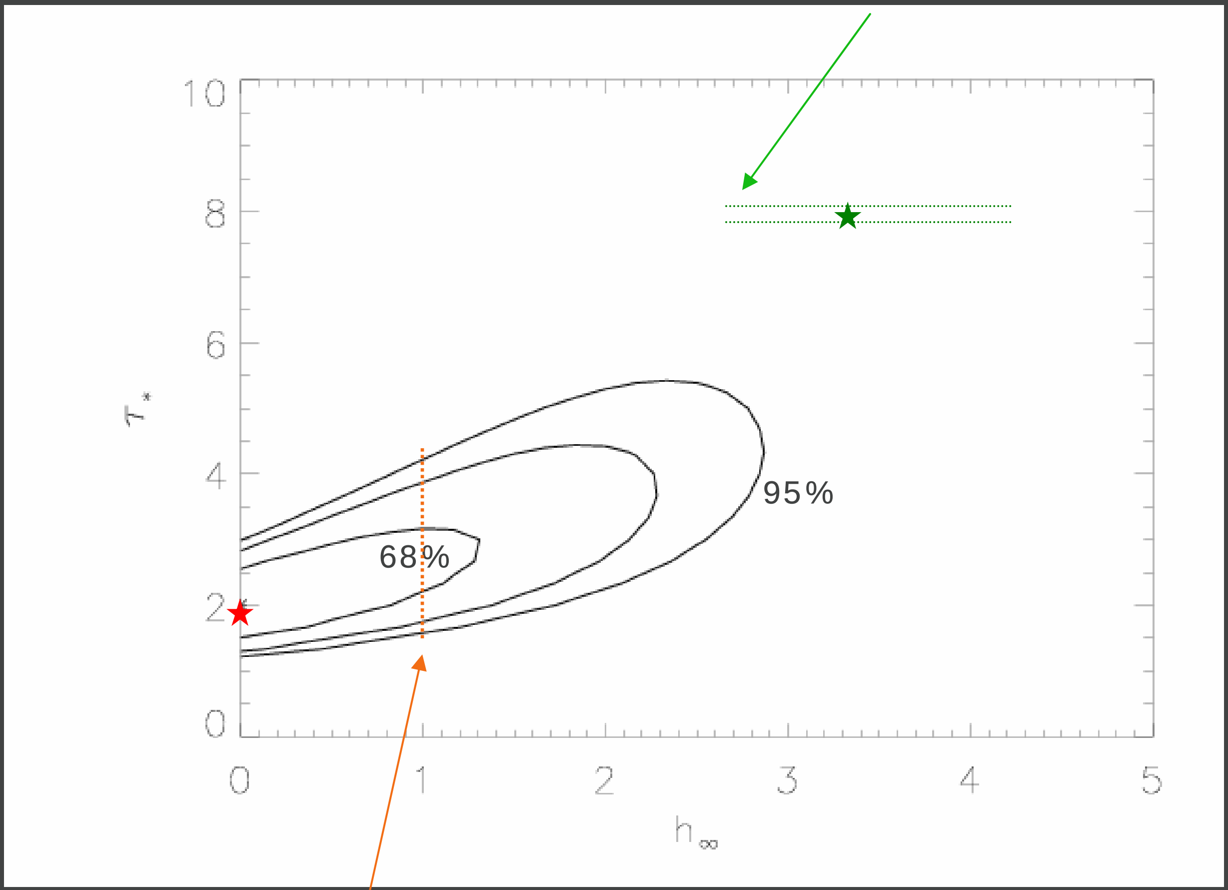

Even a model with h_∞=1 only allows for a slightly larger τ_* and, hence, mass-loss rate

This degree of porosity is ***not*** expected from the line-driven instability.

The clumping in 2-D simulations (below) is on quite *small scales*.

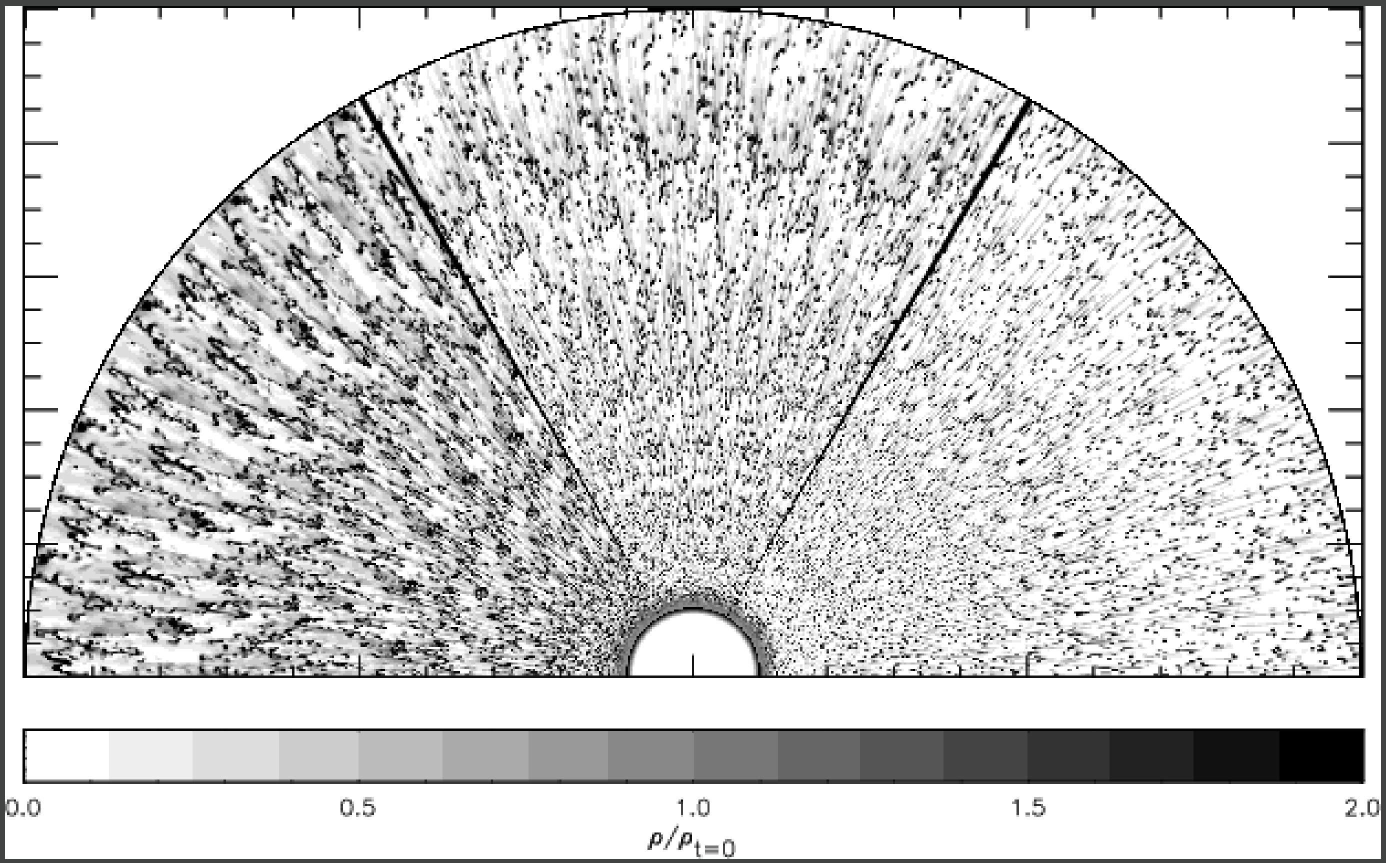

Dessart & Owocki 2003, *A&A*, 406, L1

Line profiles synthesized from the 2-D simulations shown on the previous slide (blue dashed) compared to those from a smooth wind (black solid).

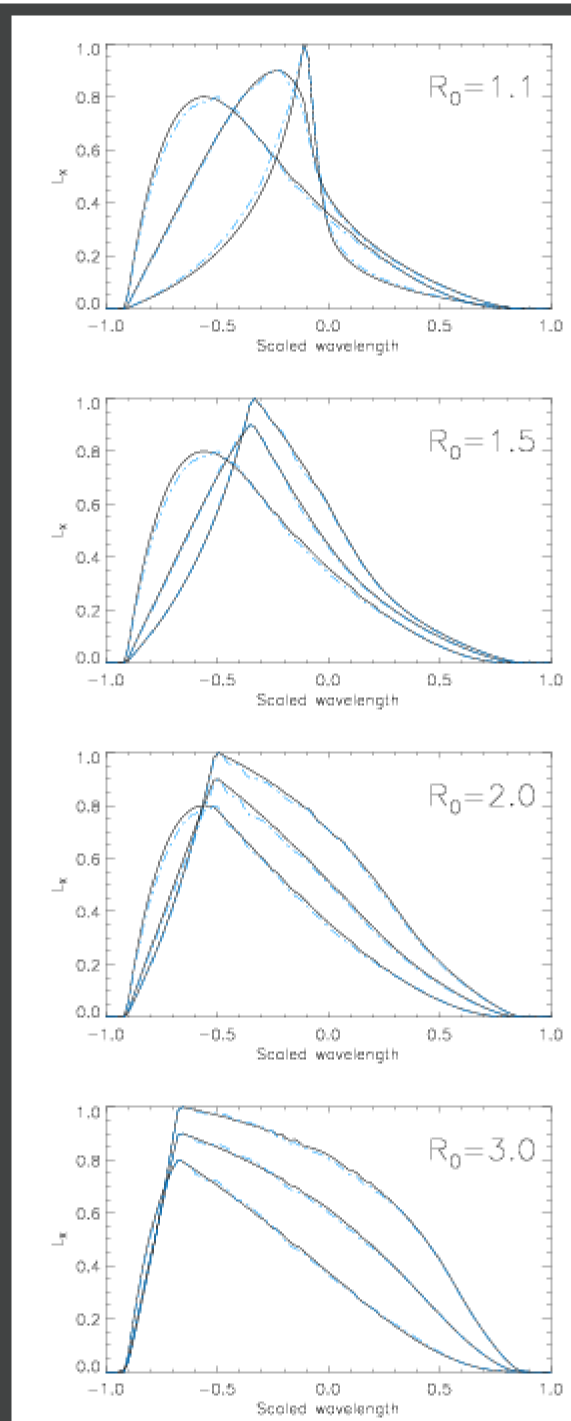

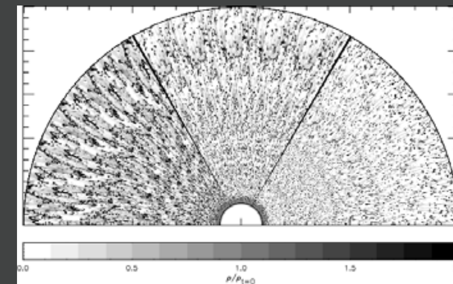

The clumping structure from state-of-the art simulations has **no effect** on the line profiles.

Each frame shows profiles calculated assuming $\tau_* = 1, 2, 5$.

Courtesy: Luc Dessart

Mass-loss rates of O stars may need to be revised downward

Several different lines of evidence:

- P V absorption (FUSE) [Fullerton et al. 2006]
- Density-squared emission – radially varying clumping (H-alpha and radio free-free) [Puls et al. 2006]
- Detailed atmosphere + wind UV modeling [Bouret et al. 2003]

Let’s look at another normal O supergiant

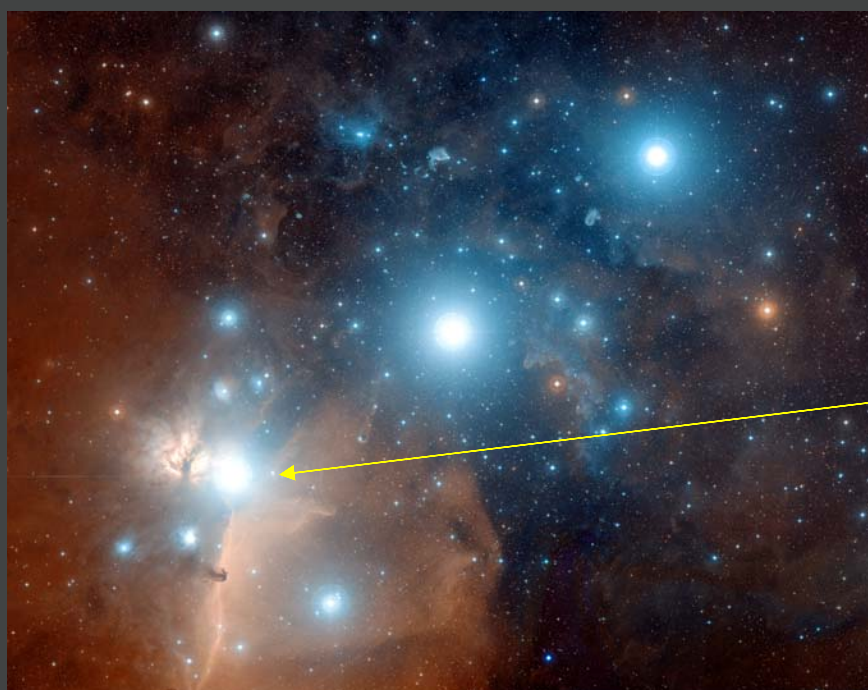

ζ Ori: *Alnitak*

O9.7 I

wind is less dense than ζ Pup’s

ζ Ori (O9.7 I) – the lines are broad, shifted, and asymmetric

An unshifted Gaussian doesn't fit

A shifted Gaussian fits OK

A kinematic, smooth wind model with absorption fits better

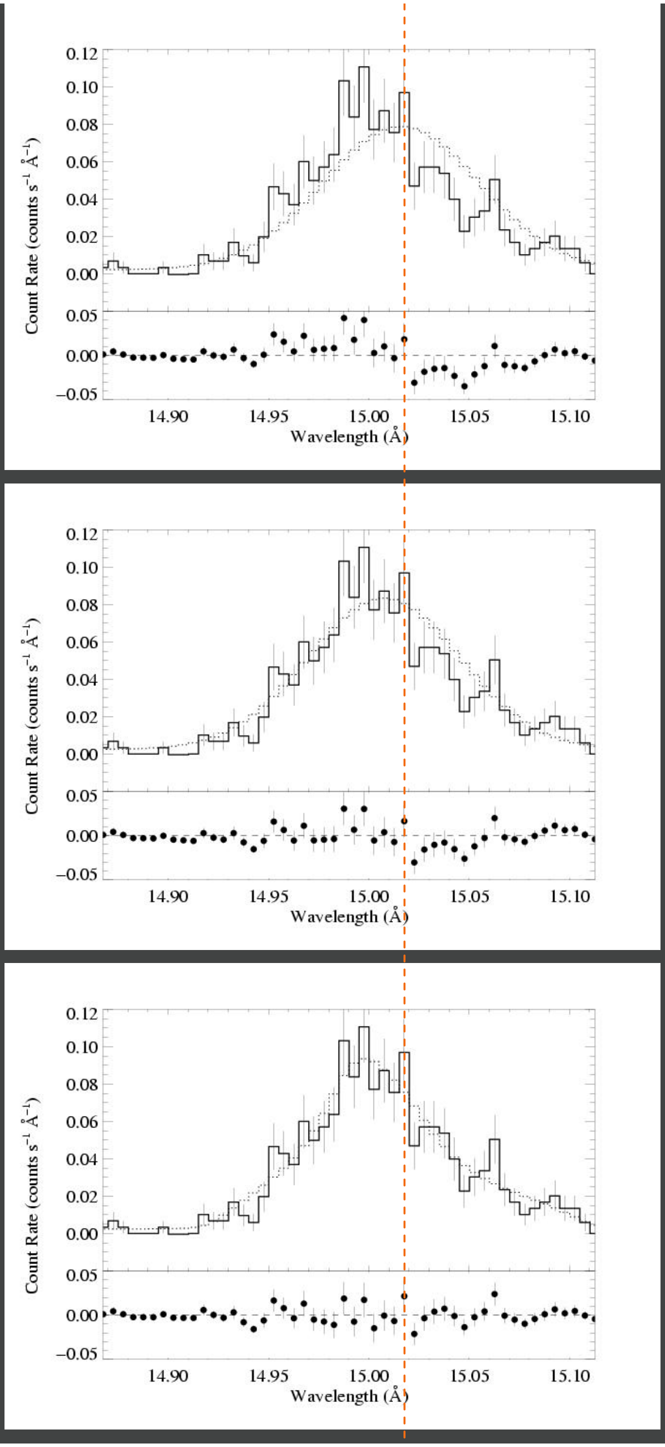

94%

73%

54%

Rejection probabilities are shown on the right of each panel.

Fit results for ζ Ori summarized

Note that the O VII line at 21.6 Å is longward of the O K-shell edge -- evidence for non-gray opacity?

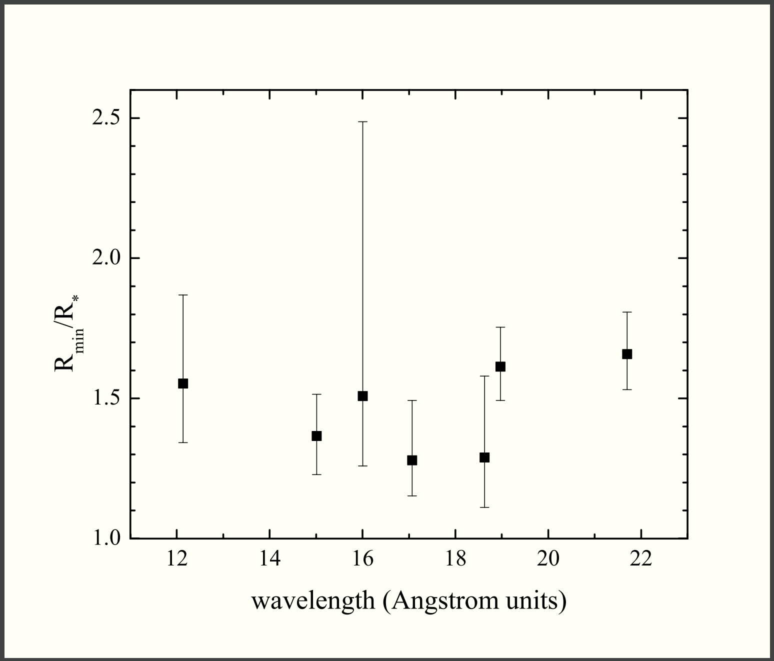

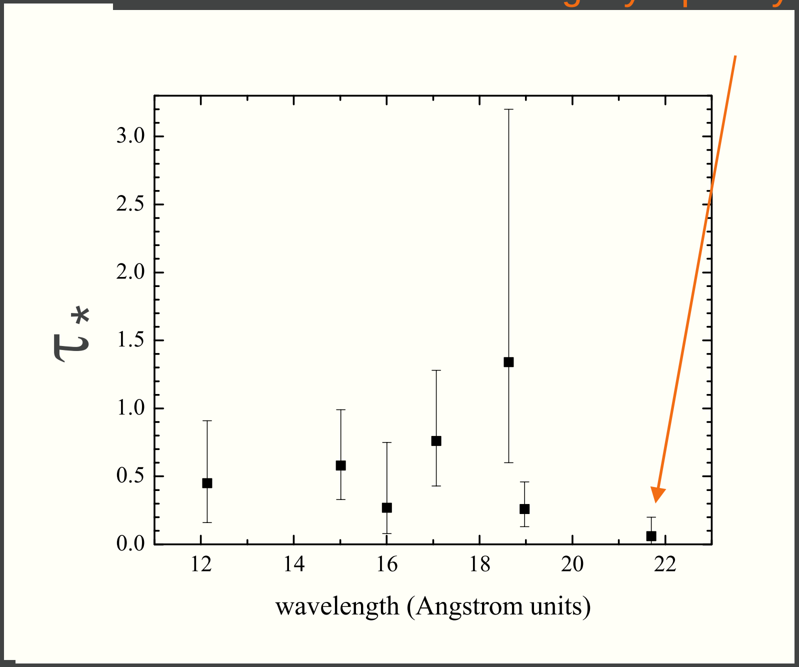

The wind optical depths are ~4 times lower than those found for ζ Pup…which is roughly consistent with the differences in stellar and wind parameters between the two stars

Data indicate that the effective opacity is gray:
all the profiles in a given star's X-ray spectrum look the same

This is explained naturally by a porosity-dominated wind;

But, atomic opacity is also quite gray over the relevant wavelength range.

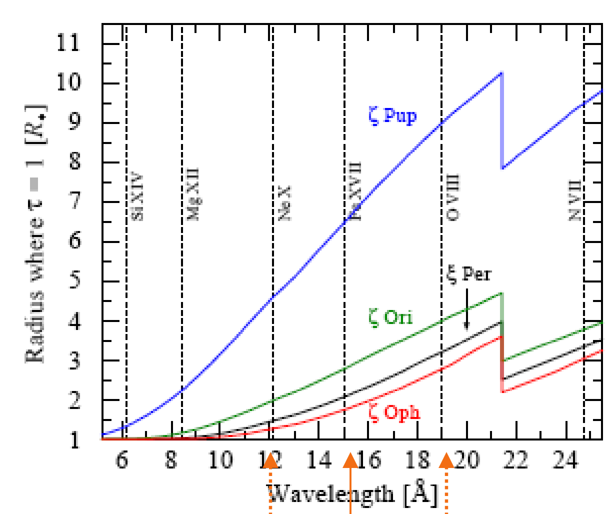

Figure 5. The radius were the radial optical depth of the wind becomes unity in dependence on the wavelength in the Chandra HETGS/MEG range. The calculations were done using the POWR stellar atmosphere code (see text) with stellar parameters from Table 2. The prominent edge at λ 21.5 Å is due to oxygen. The vertical dashed lines correspond to the wavelengths of the studied lines (as indicated).

OFH2006

Fe XVII @ 15 Å

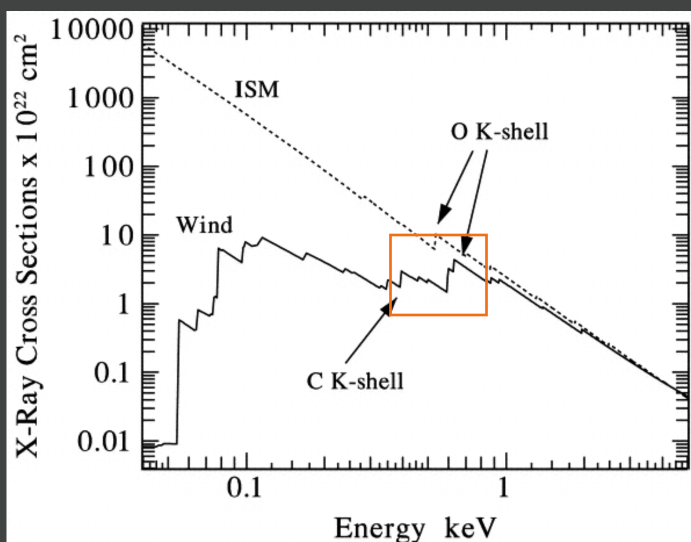

Waldron et al. 1998, *ApJS*, 118, 217

Wind opacity: bound-free, primarily from partially ionized C, N, O in the ambient wind

Each ion has maximum opacity at the photoionization threshold, with $\kappa \sim \lambda^3$...until the next edge is reached.

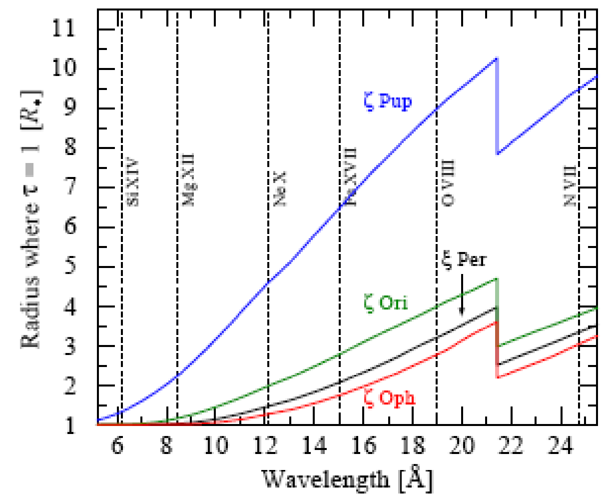

Figure 5. The radius were the radial optical depth of the wind becomes unity in dependence on the wavelength in the Chandra HETGS/MEG range. The calculations were done using the PoWR stellar atmosphere code (see text) with stellar parameters from Table 2. The prominent edge at λ 21.5 Å is due to oxygen. The vertical dashed lines correspond to the wavelengths of the studied lines (as indicated).

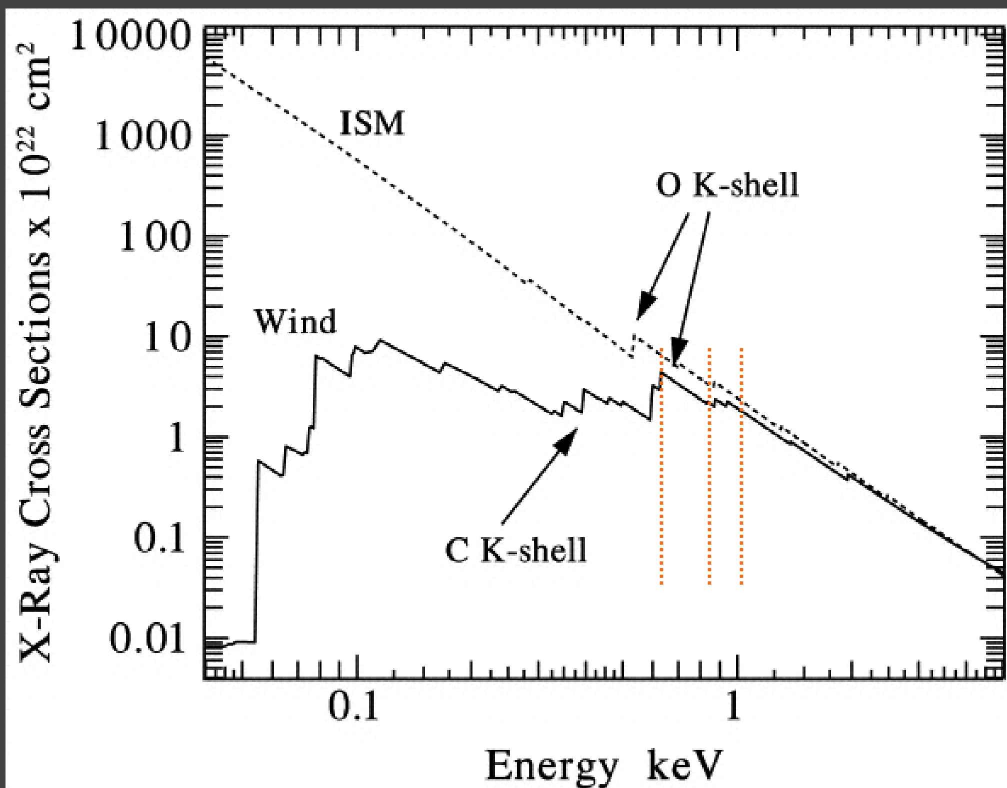

OFH2006 show only a single edge, of neutral O.

Combined effects of different elements and the shifting of edges due to ionization tend to flatten out the opacity.

Conclusions

O star X-ray emission line profiles are broadened, shifted, and asymmetric as the wind-shock scenario predicts

But the degree of asymmetry requires significantly lower wind optical depths than are expected in these stars

Clumping and the associated porosity can, in principle, alleviate this problem, but only if the degree of clumping is unrealistically high – mass-loss rate reductions of factors of several are favored

The wind-shock scenario explains the data, but O star mass-loss rates are lower than have been supposed!